Aspects of Heavy Quark Physics

Thesis by

Martin Gremm

In Partial Fulfillment of the Requirements

for the Degree of

Doctor of Philosophy

California Institute of Technology

Pasadena, California

1998

(Submitted April 7, 1998)

Acknowledgements

It is a pleasure to thank my advisor Mark Wise for his support and encouragement, many coffees, dinners and workouts. I also thank M. Aganagic, S. Cherkis, H. Davoudiasl, S. Frautschi, E. Gimon, P. Horava, E. Keski-Vakkuri, P. Kraus, T. Mehen, S. Ouellette, D. Politzer, C. Popescu, J. Preskill, J. Schwarz, I. Stewart, H. Tuck, E. Westphal as well as A. Kapustin, A. Leibovich, Z. Ligeti, D. Lowe and K. Rajagopal for contributing to the relaxed yet stimulating atmosphere. I am especially grateful to my collaborators Mina Aganagic, Eric Gimon, Anton Kapustin, Zoltan Ligeti, Iain Stewart and Mark Wise for giving me the opportunity to learn from our joint efforts. Lastly, I appreciate that Mina Aganagic, Hooman Davoudiasl, Eric Gimon, Anton Kapustin, Tom Mehen and Iain Stewart made sure that not all of my time was spent on physics.

Abstract

We discuss the use of two QCD based effective field theories in determining parameters of the standard model. Heavy Quark Effective theory provides a framework for studying the weak decays of the B meson. We calculate the $B \to X_c \ell \nu$ decay rate to second nonvanishing order in the HQET expansion and compare the theoretical prediction to experimental data. This allows us to determine the b and c pole quark masses and the weak mixing angle V_{cb}.

Nonrelativistic QCD is an effective field theory in which bound states of two heavy quarks can be analyzed conveniently. We use this approach to compute the leading relativistic corrections to the decay of S-wave quarkonia. These corrections can be expressed in terms of the leading order result and the quark pole mass. Including color octet contributions and the first relativistic corrections, we extract the value of α_s from low energy data. We also show that the color octet contributions to the decay rates are not negligible.

Contents

List of Figures

List of Tables

Chapter 1 Introduction

The standard model of particle physics is based on the gauge group $SU(3)_c \times SU(2) \times U(1)$. The $SU(3)_c$ describes the color interactions (QCD) and the $SU(2) \times U(1)$ gauge group gives rise to the electroweak interactions. Currently three families of quarks and leptons are known and additional families with light neutrinos are ruled out by the measurement of the width of the Z. The matter content of the standard model is given in Table 1.1. The tree families are labeled by $i = 1, 2, 3$, Q_L^i are the $SU(2)$ doublets of left handed quarks and L_L^i are the doublets of left handed neutrinos and electrons. When the Higgs boson, H, acquires an expectation value, it breaks the electroweak gauge symmetry, $SU(2) \times U(1)$, to $U(1)_{\rm em}$ giving rise to the electromagnetic gauge group and the massive $W^{\pm}$ and Z bosons mediating weak decays at low energies.

The description of particle physics based on this model has so far enjoyed spectacular success. To date, there are no measurements that indicate any deviation from the standard model predictions. However, to make such predictions it is necessary to know the value of the parameters that enter the model to as good an accuracy as possible. There are many such parameters: the masses of all standard model particles, three gauge couplings and the Cabibbo-Kobayashi-Maskawa matrix elements. Some of these parameters, such as the charged lepton masses, can be determined with relative ease, but many are not accessible without some understanding of the strong

Field	$SU(3)_c$	$SU(2)$	$U(1)$
$Q_L^i = (u_L^i, d_L^i)$	□	□	1/6
u_R^i	□	□	2/3
d_R^i	□	□	−1/3
$L_L^i = (\nu_L^i, e_L^i)$	1	□	−1/2
e_R^i	1	1	−1
$H = (H^+, H^0)$	1	□	1/2

Table 1.1: The matter content of the Standard Model.

interactions.

In QCD the value of the coupling constant α_s depends on the energy scale at which it is evaluated. At sufficiently high scales α_s is small and the color interactions can be described in the framework of perturbation theory. However, α_s grows as one lowers the scale until it becomes larger than one. Thus perturbation theory is not applicable in processes for which the typical scale is too low. In this regime, there is no known general method for describing physical processes in some approximation scheme such as perturbation theory. This complicates the determination of almost all properties of the fields charged under $SU(3)_c$. More precisely, the quark masses, the CKM angles and α_s are difficult to measure without a reliable theoretical framework in which nonperturbative effects can be taken into account. While no single method accomplishes this for all processes where nonperturbative effects are important, there are a number of effective field theories that describe QCD in some limit. Chiral perturbation theory can be used to calculate processes involving only light mesons as well as the interactions between heavy and light mesons, provided the momentum of the light mesons is not too large. Heavy Quark Effective Theory (HQET) furnishes a framework in which the decays of mesons containing one heavy quark can be described as an expansion in the inverse heavy quark mass and, finally, Nonrelativistic QCD (NRQCD) is an effective field theory that describes the production and decays of bound states of two heavy quarks. All of these effective field theories provide systematic approximations to some limit of QCD, which allows one to make reliable theoretical predictions for processes involving nonperturbative effects. This makes it possible to extract parameters such as the quark masses, the CKM angles and α_s with controllable uncertainties.

The standard model is generally believed to be a low energy effective theory of some larger, perhaps more symmetric theory at higher energies. If this is true, there must be a scale at which the high energy theory is matched onto the effective theory. All the parameters of the standard model can then be expressed in terms of the fewer parameters of the microscopic theory. There will also be new interactions mediated by nonrenormalizable terms in the standard model Lagrangian. These terms are sup-

pressed by powers of the scale at which new physics appears. A precise measurement of the standard model parameters will ultimately lead to the discovery of contributions from these higher dimension operators in the Lagrangian. Since these operators will presumably contribute in different ways to different decays, one should be able to see discrepancies in the value of standard model parameters determined from several different experiments. These deviations would indicate the presence of additional interactions. A successful microscopic theory behind the standard model would have to predict not only the values of the standard model parameters but also the additional contributions to measurable processes that stem from the higher dimension operators. It turns out that constructing a theory that reproduces the standard model at low energies with parameters that are not ruled out by experiments is very difficult and it will become more so as these parameters are measured more and more accurately.

In this thesis we will describe how certain observables constructed from the electron energy spectrum in inclusive $B \to X_c \ell \nu$ decays can be used to constrain the parameters that appear in HQET at next to leading order. Both the normalization and the shape of the electron spectrum are modified by nonperturbative corrections. It will turn out that observables that are sensitive to the shape rather than the normalization provide the most stringent constraints on the values of the HQET matrix elements that appear in the theoretical predictions for the semileptonic decay rates. Once the numerical value of these a priori unknown parameters is determined, one can use them to extract the masses of the b and c quarks, the CKM angle $|V_{cb}|$ and make more precise predictions for other processes that can be studied in the framework of HQET. The focus here will be on inclusive decays of the B meson because in this case one does not need a detailed knowledge of the properties of the individual charmed final states to make predictions. A similar analysis can also be done using exclusive channels, but in that case the decay processes are described in terms of one or more unknown functions (the Isgur-Wise functions) rather than in terms of a small number of expectation values of HQET operators. This complicates making accurate predictions but this is compensated in part by much better experimental data on these decays. Thus, at least for the extraction of $|V_{cb}|$, exclusive decays are

a very competitive approach.

We will also describe how NRQCD can be used to obtain expressions for the decay rates of S-wave quarkonia to two leptons or light hadrons, including the first relativistic corrections. The dominant contributions to these decays come from the annihilation of quark anti-quark bound states in a color singlet state, but there are color octet contributions as well. We will show that both the color octet contributions and the relativistic corrections are important by comparing the NRQCD predictions with and without including the color octet contributions to the experimentally measured numbers. The relativistic corrections can be expressed in terms of the leading order matrix elements and the binding energy of the quarkonium state. This provides a way to evaluate them quantitatively. We use this to extract the value of α_s at m_b from experimental data and compare it to the high energy value measured at LEP. Our extraction provides a value of α_s that is compatible with the LEP result, indicating that that there may not be any disagreement between high and low energy extractions of α_s.

In Chapter 2 we describe HQET as an effective theory and show how one can pass from the QCD Lagrangian to the effective Lagrangian in a controlled way. We also describe the Operator Product Expansion (OPE) needed to calculate inclusive semileptonic B decay rates including nonperturbative corrections. The perturbative corrections to this decay are the subject of Chapter 3. In Chapter 4 we use the results of the previous two chapters to extract the values of the lowest dimension HQET matrix elements from experimental data and discuss the theoretical uncertainties in this extraction from higher order nonperturbative corrections. In Chapter 5 we leave HQET and switch to a discussion of the decays of S-wave quarkonia in the framework of NRQCD. The expressions for the annihilation rates are computed to first subleading order in the nonrelativistic expansion. We show that it is necessary to include color octet contributions for the NRQCD predictions to agree with experimental data. Including both relativistic corrections and the color octet contribution, we use our results to extract the value of α_s from experimental data. In Chapter 6 we make some concluding remarks and summarize our results.

Chapter 2 Heavy Quark Effective Theory

2.1 Heavy Quark Symmetry

Heavy Quark Symmetry is an approximate symmetry of the heavy quark in a bound state with one (or more) light quarks [1]. In the restframe of the meson (or baryon), the heavy quark is almost at rest. This can be seen as follows: the light degrees of freedom have a momentum of order Λ_{QCD}, the strong coupling scale of QCD. This implies that the momentum of the heavy quark is also of the same order $P_Q = m_Q v = \Lambda_{QCD}$. If the mass of the heavy quark is much larger than the strong coupling scale Λ_{QCD}, v is very small and the heavy quark is almost at rest. Taking the limit $m_Q \to \infty$, we can treat the heavy quark as a static source of a color field the light degrees of freedom propagate in. This implies that we can exchange an infinitely heavy quark with another of a different flavor without changing the color field the light degrees of freedom feel. This is the flavor symmetry of the heavy quarks that is part of the Heavy Quark Symmetry (HQS). The second part of it is the spin symmetry. Since the chromomagnetic moment of a quark is inversely proportional to its mass, the interactions with the light degrees of freedom become independent of the heavy quark spin in the limit of infinitely heavy quarks. Thus we find that the behavior of the light degrees of freedom does not depend on the flavor or the spin orientation of the heavy quark. The HQS symmetry group is $U(2N_f)$. The generators of this group permute the heavy quark flavor and spin. In practice, only the b and c quarks are heavy enough for this symmetry to be a good approximation. The top quark, although certainly heavy enough, decays before it can hadronize, which takes it outside the realm of applicability of HQET.

These symmetries are not explicit in the QCD Lagrangian,

$$\mathcal{L} = \bar{Q}\left(i\not{D} - m_Q\right)Q, \tag{2.1}$$

and in this form it does not lend itself to taking the $m_Q \to \infty$ limit. To make the full $U(2N_f)$ symmetry explicit, it is convenient to pass to an effective field theory. The momentum of the heavy quark inside a meson moving with velocity v can be decomposed as $P = m_Q v + k$ where the first term comes from the motion of the meson and $k \approx \Lambda_{QCD}$ is the residual motion of the heavy quark induced by interactions with the light degrees of freedom. Decomposing the heavy quark field in the Lagrangian Eq. (2.1) as

$$h_v = e^{im_Q v\cdot x} P_+ Q(x) \tag{2.2}$$

$$H_v = e^{im_Q v\cdot x} P_- Q(x). \tag{2.3}$$

where $P_+ = (1+\not{v})/2$ and $P_- = (1-\not{v})/2$ amounts to factoring out the center of mass motion of the meson and splitting the Dirac spinor representing the full QCD quark field into its upper and lower component. Note that a covariant derivative acting on h_v will bring down a power of the residual momentum of the heavy quark in the meson, rather than its total momentum. Because of the projection operators $P_\pm$, the field in Eq. (2.2) satisfies $\not{v} h_v = h_v$ and $\bar{h}_v \gamma^\mu h_v = v^\mu \bar{h}_v h_v$. Substituting

$$Q(x) = e^{-im_Q v\cdot x}[h_v(x) + H_v(x)], \tag{2.4}$$

back into the Lagrangian, Eq. (2.1), gives

$$\mathcal{L} = \bar{h}_v iv\cdot D h_v - \bar{H}_v(iv\cdot D + 2m_Q)H_v + \bar{h}_v i\not{D}_\perp H_v + \bar{H}_v i\not{D}_\perp h_v, \tag{2.5}$$

where

$$D_\perp^\mu = D^\mu - v^\mu v\cdot D. \tag{2.6}$$

In this Lagrangian, the antiquark field H_v has mass $2m_Q$ and the quark field h_v is massless. We can integrate out the heavy field H_v which results in the effective Lagrangian

$$\mathcal{L}_{eff} = \bar{h}_v iv\cdot D h_v + \bar{h}_v i\not{D}_\perp \frac{1}{iv\cdot D + 2m_Q - i\epsilon} i\not{D}_\perp h_v. \tag{2.7}$$

For this expression to make sense, the propagator in the second term should be expanded in powers of $1/m_Q$. To second order in $1/m_Q$ this expansion reads [2, 3, 4, 5]

$$\begin{aligned}\mathcal{L}_{eff} &= \bar{h}_v iv\cdot D h_v + \frac{1}{2m_Q}\bar{h}_v (iD_\perp)^2 h_v + \frac{g_s}{4m_Q}\bar{h}_v \sigma_{\alpha\beta} G^{\alpha\beta} h_v \\ &- \frac{1}{4m_Q^2}\bar{h}_v\, i\not{D}_\perp (iv\cdot D) i\not{D}_\perp\, h_v + \frac{1}{8m_Q^2}\bar{h}_v\,(i\not{D}_\perp)^2 (iv\cdot D)\, h_v \\ &+ \frac{1}{8m_Q^2}\bar{h}_v\,(iv\cdot D)(i\not{D}_\perp)^2\, h_v + \mathcal{O}(\frac{1}{m_Q^3}).\end{aligned} \tag{2.8}$$

In the limit $m_Q \to \infty$ only the first term survives. Since the operator $iv\cdot D$ does not contain any gamma matrices, the first term is manifestly invariant under transformations on the heavy quark spin. The effective Lagrangian above contains only one flavor of quarks but it can be extended to include N_f flavors, all moving with the same velocity v

$$\mathcal{L}_{eff} = \sum_{i=1}^{N_f} \bar{h}_v^i iv\cdot D h_v^i. \tag{2.9}$$

This Lagrangian is manifestly invariant under $U(2N_f)$ transformations on the heavy quark fields.

The terms suppressed by powers of $1/m_Q$ break heavy quark symmetry. The first correction term does not contain any gamma matrices and therefore commutes with any transformation on the spin of the heavy quark. However, since it contains an explicit quark mass, it breaks flavor symmetry. The second term breaks both the flavor and the spin symmetry. If these symmetry breaking terms are sufficiently small, or conversely the quark sufficiently heavy, they can be treated as small perturbations. This leads to an expansion in powers of Λ_{QCD}/m_Q of any quantity computed using this Lagrangian.

The Lagrangian, Eq. (2.8), was obtained from tree level considerations. In general there will be perturbative corrections to the coefficients of the operators in the Lagrangian. These can be obtained by comparing perturbative calculations of suitable processes in full QCD and in HQET. Demanding that the results agree after expansion in inverse powers of the quark mass determines the matching coefficients.

This has been done for the two dimension five operators in Eq. (2.8). This part of the Lagrangian gets modified to

$$\mathcal{L}_5 = \frac{C_{kin}}{2m_Q}\bar{h}_v\,(iD_\perp)^2\,h_v + \frac{C_{mag}}{2m_Q}\bar{h}_v\,\frac{g}{2}\,\sigma_{\mu\nu}\,G^{\mu\nu}\,h_v, \tag{2.10}$$

where $C_{kin} = 1$ to all orders in perturbation theory [6] and after summing up the logarithms of the form $\alpha_s^n \log^n \frac{\mu}{m_Q}$ [7]

$$C_{mag}(\mu) = \left(\frac{\alpha_s(m_Q)}{\alpha_s(\mu)}\right)^{3/\beta_0}\left(1 + \frac{13}{6}\frac{\alpha_s}{\pi}\right). \tag{2.11}$$

Here the one loop beta function is given by $\beta_0 = 11 - 2n_f/3$. No such calculation has been done for the higher dimension operators in the Lagrangian but for our purposes knowing the tree level coefficients will be sufficient. In general, one should expect all operators that are consistent with the symmetries of QCD to appear when the matching of full QCD and HQET is extended to higher loops. The leading piece of the coefficients of such operators would then be of order α_s^n for some $n \geq 1$.

Integrating out the heavy anti-quark field H_v induces correction terms in the relation between the heavy quark field h_v and the full QCD field Q. Eq. (2.4) is modified to [5]

$$Q(x) = e^{-im_Q v\cdot x}\left(1 + \frac{i\not{D}_\perp}{2m_Q} + \frac{(v\cdot D)\not{D}_\perp}{4m_Q^2} - \frac{\not{D}_\perp^2}{8m_Q^2} + \mathcal{O}\left(\frac{1}{m_Q^3}\right)\right)h_v(x). \tag{2.12}$$

In this definition we have used the freedom to redefine the field h_v to choose it such that it satisfies the usual equal time commutation relations. The fields defined in this way are the usual Foldy-Wouthuysen fields familiar from the nonrelativistic expansion of the Dirac equation.

The effective theory we have constructed above describes a heavy quark in a bound state with light quarks. It is ideally suited for describing the weak decay of the heavy quark inside the meson to another heavy quark. If both quarks are infinitely heavy, this decay simply amounts to replacing the initial quark by another of a different

flavor. As we have seen, this operation is part of the symmetry transformations under which the leading order Lagrangian of HQET is invariant. If the initial and final quark both have a finite mass much larger than Λ_{QCD}, the $1/m_Q$ corrections need to be taken into account [3, 4].

Although we will not use this aspect of HQS, it is worth mentioning that in the infinite mass limit, HQS allows one to relate the form factors in $B \to D^{(*)}$ transitions to a single unknown function, the Isgur-Wise function [1]. For quarks with finite mass, a number of additional form factors appear, making the HQS based predictions less stringent. A second application of heavy quark spin symmetry can be found in Chapter 5, where it is used to reduce the number of independent NRQCD matrix elements.

In inclusive decays, on the other hand, the finite mass corrections are encoded in the matrix elements of HQET operators, i.e., one has to deal with unknown numbers rather than with unknown functions. There are no corrections to total and differential semileptonic decay rates at order $1/m_Q$ and the $1/m_Q^2$ corrections can be parametrized by two nonperturbative matrix elements [3, 4]. The matrix elements are universal, i.e., once their value IS KNOWN, they can be used to make predictions for any process that can be described by the Lagrangian Eq. (2.8). The determination of these matrix elements [8, 9, 10] is part of the subject of this thesis.

2.2 The semileptonic decay $B \to X_c \ell \nu$

In this section we give a detailed description of how the $1/m_Q$ expansion can be used to obtain expressions for the differential decay rates in $b \to c\ell\bar{\nu}$ decays, including nonperturbative corrections. In Chapter 4 we will use the shape of the differential rates to extract the values of the HQET matrix elements parametrizing the nonperturbative corrections. For that purpose, it will turn out to be useful to consider the charged lepton spectrum and the invariant mass spectrum of the final state hadrons. In this chapter we provide expressions for both, including the nonperturbative corrections that appear at order $1/m_Q^3$. Although we are mainly interested in extracting

the values of matrix elements that appear at order $1/m_Q^2$, we will need the $1/m_Q^3$ corrections to estimate the theoretical uncertainties.

Since the b quark is much lighter than the W bosons, we can pass to an effective theory of the weak interactions by integrating out the Ws. This results in the usual four-fermion interactions that are the remnant of the W exchange in the full theory. The interaction term in the effective Hamiltonian density responsible for $b \to c\ell\bar{\nu}$ decays is

$$H_W = -V_{cb}\frac{4G_F}{\sqrt{2}} J^\mu J_{\ell\mu}, \tag{2.13}$$

where $J^\mu = \bar{c}_L \gamma^\mu b_L$ is the left-handed quark current, and $J_\ell^\mu = \bar{\ell}_L \gamma^\mu \bar{\nu}_L$ is the left-handed lepton current. In the analysis presented here we will neglect higher order electroweak corrections to the decay rate. Then the amplitude for $b \to c\ell\bar{\nu}$ factorizes into a leptonic part, which can be evaluated exactly and a hadronic part which receives nonperturbative corrections. The leptonic part is given in terms of the lepton tensor

$$L_{\mu\nu} = Tr\left[(\not{P}_\ell + m_\ell)\gamma_\mu(1-\gamma^5)\not{P}_\nu\gamma_\nu(1-\gamma^5)\right] \tag{2.14}$$

and the hadronic part of the amplitude is determined by the hadronic tensor

$$W^{\mu\nu} = (2\pi)^3 \sum_{X_c} \delta^4\left(p_B - q - p_{X_c}\right) \langle B(v)|J^{\nu\dagger}|X_c\rangle\langle X_c|J^\mu|B(v)\rangle. \tag{2.15}$$

Here $q = P_\ell + P_\nu$. The hadron tensor can be expanded in terms of five form factors

$$W^{\mu\nu} = -g^{\mu\nu}W_1 + v^\mu v^\nu W_2 - i\epsilon^{\mu\nu\alpha\beta}v_\alpha q_\beta W_3 + q^\mu q^\nu W_4 + (q^\mu v^\nu + q^\nu v^\mu)W_5, \tag{2.16}$$

where the form factors W_i are functions of q^2 and $v\cdot q$. In terms of these form factors, the differential semileptonic decay rate is given by

$$\begin{aligned}\frac{d\Gamma}{dq^2 dE_\ell dE_\nu} &= \frac{96\,\Gamma_0}{m_b^5}\left(W_1\,q^2 + W_2\left(2E_\ell E_\nu - \frac{1}{2}q^2\right) + W_3\,q^2\,(E_\ell - E_\nu)\right) \\ &\quad \times\theta(E_\ell)\,\theta(E_\nu)\,\theta(q^2)\,\theta(4E_\ell E_\nu - q^2).\end{aligned} \tag{2.17}$$

Here Γ_0 is the spectator model total decay rate in the limit of zero charm mass

$$\Gamma_0 = |V_{cb}|^2 G_F^2 \frac{m_b^5}{192\pi^3}, \tag{2.18}$$

and we have neglected the lepton mass.

The hadron tensor, Eq. (2.15), contains matrix elements of the quark current between meson states. These quantities can be evaluated in terms of Isgur-Wise functions for each charmed hadron in the final state individually. However, since we are interested in the inclusive rate, we can perform the sum over the final states and relate the hadron tensor to the current correlator $T^{\mu\nu}$

$$\begin{aligned} T^{\mu\nu} &= -i \int d^4x e^{-iq\cdot x} \langle B(v)|T\left[J^{\nu\dagger}(x) J^{\mu}(0)\right]|B(v)\rangle \\ &= -g^{\mu\nu}T_1 + v^\mu v^\nu T_2 - i\epsilon^{\mu\nu\alpha\beta} v_\alpha q_\beta T_3 + q^\mu q^\nu T_4 + (q^\mu v^\nu + q^\nu v^\mu) T_5. \end{aligned} \tag{2.19}$$

As indicated above, this correlator also has an expansion in terms of five form factors T_i that are in one-to-one correspondence with the form factors W_i in Eq. (2.16). The analytic structure of $T^{\mu\nu}$ in the $v \cdot q$ plane is shown in Fig. 2.1. The two cuts correspond to the two possible time orderings of the currents in Eq. (2.19). As one can see by inserting a complete set of states into the current correlator, only the left cut corresponds to physical final states. The right cut corresponds to states with two b quarks which clearly are irrelevant for the B decays we are studying here. We can view W, Eq. (2.15), as the discontinuity across the physical cut: $W_i = -\frac{1}{\pi}\mathrm{Im}T_i$. This can also be seen by inserting a complete set of states between the currents in Eq. (2.19). By virtue of this relation between $T^{\mu\nu}$ and $W^{\mu\nu}$, computing the current correlator in a controlled expansion amounts to computing the form factors W_i.

Away from the physical cut, $T^{\mu\nu}$ can be computed using the Operator Product Expansion [11]. Here the idea is to expand the nonlocal correlator of two quark currents in Eq. (2.19) in terms of an infinite sum of local operators $\mathcal{O}_i$ multiplied by

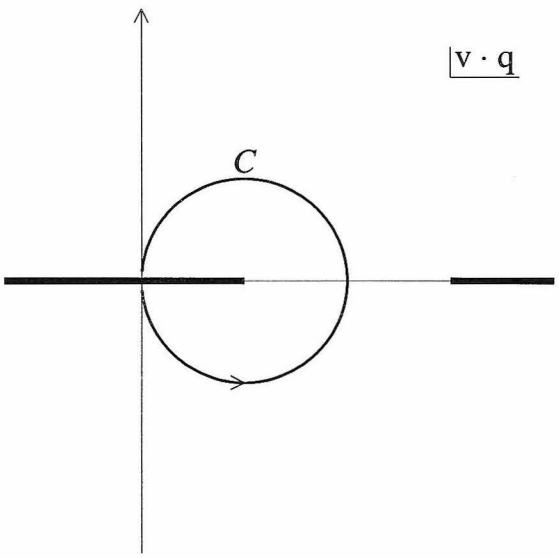

Figure 2.1: The analytic structure of the current correlator $T^{\mu\nu}$ in the $q \cdot v$ plane

Wilson coefficients C_i

$$T\left[J^{\nu\dagger}(x)J^{\mu}(0)\right] = \sum_i C_i(x)\mathcal{O}_i(0). \tag{2.20}$$

In general, this series will not converge, but if we choose q such that all intermediate states are far off shell, the sum on the rhs of Eq. (2.20) is expected to be dominated by the lowest dimension operators. Thus we can evaluate the current correlator approximately everywhere along the contour C in Fig. 2.1 as long as it stays away from the physical cut. Recall that the hadron tensor W is given by the discontinuity across the physical cut in the $v \cdot q$ plane. Since $T^{\mu\nu}$ is analytic in the $v \cdot q$ plane except for the two cuts, we can deform the integration contour needed to evaluate this discontinuity to look like C in Fig. 2.1 without changing the value of the contour integral. This allows us to compute the hadron tensor in terms of the expectation values of the rhs of Eq. (2.20) if we ignore the uncertainty in the integral coming from the point where the contour C touches the cut. The OPE does not reproduce the differential decay rates point-by-point. Varying q^2 corresponds to varying the invariant mass of the hadronic final state in the semileptonic B decay. For low hadronic masses this

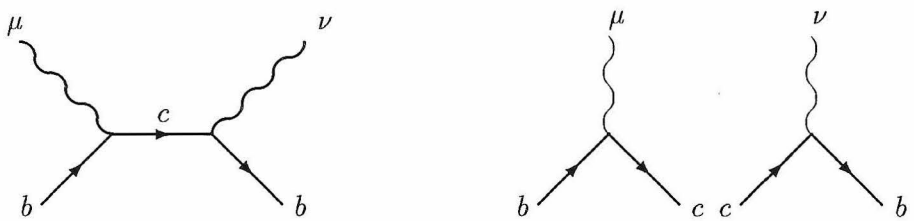

Figure 2.2: (a) The relevant term in the operator product expansion. Wavy lines denote the insertions of left-handed currents. (b) does not contribute to $b \to c$ decay.

spectrum has pronounced and well separated resonances. However, in the parton picture underlying the OPE, these resonances are not visible. Global quark-hadron duality is the statement that after integrating over a sufficiently large region in the hadronic invariant mass spectrum, the parton picture of the OPE and the integral over the resonances will give the same result. Thus we expect the OPE calculation to be valid only if we integrate over the low invariant mass spectrum. For higher invariant masses, the resonances are less pronounced and closer together. The parts of differential rates that correspond to this part of the mass spectrum can be expected to be accurate point-by-point.

For our purposes it will be sufficient to calculate the Wilson coefficients C_i of all but the leading operator at tree level. The only diagram which has a discontinuity across the physical cut is shown in Fig. 2.2a. The corresponding contribution to the time-ordered product is

$$\begin{aligned} &\bar{b}\gamma^\nu P_L \frac{1}{m_b \not{v} - \not{q} + i\not{D} - m_c} \gamma^\mu P_L b \qquad (2.21) \\ &= \frac{1}{\Delta_0} \bar{b}\gamma^\nu P_L \left(m_b \not{v} - \not{q} + i\not{D} + m_c\right) \sum_{n=0}^{\infty} \left(\frac{D^2 - 2(m_b v - q)\cdot iD + \frac{1}{2} g\sigma_{\alpha\beta} G^{\alpha\beta}}{\Delta_0} \right)^n \gamma^\mu P_L b, \end{aligned}$$

where $P_L = \frac{1}{2}(1 - \gamma_5)$ is the left-handed projector, $\Delta_0 = (m_b v - q)^2 - m_c^2 + i0$, D

is the covariant derivative, and we used $D_\mu D_\nu - D_\nu D_\mu = igG_{\mu\nu}$. The field $b(x)$ in Eq. (2.21) is related to the normal QCD field by $b_{\rm QCD}(x) = e^{-im_b v\cdot x} b(x)$. There are other contributions in the OPE of two currents, e.g., the one in Fig. 2.2b. However, these operators do not contribute to the decay rate once sandwiched between the B-meson states. For the diagram in Fig. 2.2b this is ensured by m_c being much larger than the available energy in the "brown muck," which is of order Λ_{QCD}.

Our calculation of the form factors T_i follows the method of Ref. [3]. We expand Eq. (2.21) to third order in D. The term with no derivatives is proportional to the conserved current $\bar{b}\gamma_\mu b$, and thus its diagonal matrix elements can be evaluated exactly in full QCD. All other contributions we express in terms of the field h_v in the effective theory and reexpand the resulting expressions in powers of $1/m_b$. Therefore, we need the expression for $b(x)$ in terms of $h_v(x)$ only to order $1/m_b^2$:

$$b(x) = \left(1 + \frac{i\not{D}_\perp}{2m_b} + \frac{(v\cdot D)\not{D}_\perp}{4m_b^2} - \frac{\not{D}_\perp^2}{8m_b^2} + \cdots\right) h_v(x), \tag{2.22}$$

where $D_\perp = D - v(v\cdot D)$. We choose to work with Foldy-Wouthuysen-type fields, because this ensures that they satisfy the usual equal-time commutation relations [5].

To evaluate the expectation values of the heavy quark bilinears, we need the equations of motion in the effective theory to order $1/m_b^2$ [5, 12]:

$$iv\cdot D h_v = \left(\frac{1}{2m_b}\not{D}_\perp^2 - \frac{i}{4m_b^2}\not{D}_\perp (v\cdot D)\not{D}_\perp + \frac{i}{8m_b^2}\left(\not{D}_\perp^2 (v\cdot D) + (v\cdot D)\not{D}_\perp^2\right) + \cdots\right) h_v. \tag{2.23}$$

By virtue of Eq. (2.23) there are no nonperturbative corrections to the form factors T_i at order $1/m_b$ [2, 3, 4]. The contributions at order $1/m_b^2$ are expressed in terms of the matrix elements

$$\begin{aligned} K_b &= -\frac{1}{2m_b^2}\langle B(v)\,|\bar{h}_v\,(iD_\perp)^2\,h_v|\,B(v)\rangle, \\ G_b &= -\frac{1}{2m_b^2}\langle B(v)\,|\bar{h}_v\,\frac{g}{2}\,\sigma_{\mu\nu}\,G^{\mu\nu}\,h_v|\,B(v)\rangle. \end{aligned} \tag{2.24}$$

The states in these matrix elements have an implicit dependence on m_b. At order

$1/m_b^2$ this dependence can be neglected, in which case these matrix elements may be expressed in terms of the mass independent matrix elements

$$\lambda_1 = \langle H_\infty(v) \,|\, \bar{h}_v \, (iD_\perp)^2 \, h_v \,|\, H_\infty(v)\rangle \tag{2.25}$$

$$\lambda_2 = \frac{1}{d_H} \langle H_\infty(v) \,|\, \bar{h}_v \, \frac{g}{2} \, \sigma_{\mu\nu} \, G^{\mu\nu} \, h_v \,|\, H_\infty(v)\rangle. \tag{2.26}$$

Here h_v is the quark field in the heavy quark effective theory. $|\, H_\infty(v)\rangle$ is the pseudoscalar ($d_P = 3$) or vector ($d_V = -1$) heavy meson state in the infinite quark mass limit [3, 4, 13], with normalization $\langle H_\infty(v) \,|\, H_\infty(v')\rangle = (2\pi)^3 v^0 \delta^{(3)}(p - p')$. The scale dependent [7] matrix element λ_2 can be obtained from the measured $B^* - B$ mass splitting, $\lambda_2(m_b) \simeq 0.12\,\mathrm{GeV}^2$. Since we will be interested in $1/m_b^3$ corrections to various observables, we need to take the m_b dependence of the B meson states in the full theory into account. In this section we will simply express all results in terms of K_b, G_b and defer the discussion of the expansions of the states to the next section.

The $1/m_b^3$ contributions to the form factors T_i from local operators can be parametrized by two matrix elements, ρ_1 and ρ_2 [14], which are related to the matrix elements ρ_D^3 and ρ_{LS}^3 introduced in Ref. [12] by $\rho_1 = \rho_D^3, \rho_2 = \frac{1}{3}\rho_{LS}^3$. They are defined as

$$\langle H_\infty(v)|\bar{h}_v(iD_\alpha)(iD_\mu)(iD_\beta)h_v|H_\infty(v)\rangle = \tfrac{1}{3}\rho_1 \, (g_{\alpha\beta} - v_\alpha v_\beta) \, v_\mu, \tag{2.27}$$

$$\langle H_\infty(v)|\bar{h}_v(iD_\alpha)(iD_\mu)(iD_\beta) \, \gamma_\delta\gamma_5 \, h_v|H_\infty(v)\rangle = \tfrac{1}{6} d_H \rho_2 \, i\epsilon_{\nu\alpha\beta\delta} v^\nu v_\mu. \tag{2.28}$$

The expectation value of any bilinear operator with three derivatives can be expressed in terms of ρ_1 and ρ_2:

$$\langle H_\infty(v)|\bar{h}_v\Gamma(iD_\alpha)(iD_\mu)(iD_\beta)h_v|H_\infty(v)\rangle = \tag{2.29}$$
$$\tfrac{1}{6}\rho_1 \, (g_{\alpha\beta} - v_\alpha v_\beta) \, v_\mu Tr\left[P_+\Gamma\right] - \tfrac{1}{12} d_H \rho_2 \, i\epsilon_{\nu\alpha\beta\delta} v^\nu v_\mu Tr\left[P_+\gamma^\delta\gamma_5 P_+\Gamma\right],$$

where $P_+ = \frac{1}{2}(1 + \not{v})$, and Γ is any four-by-four matrix.

At leading order in the $1/m_b$ expansion of Eq. (2.21), we can compute all expectation values exactly. This results in the leading order form factors

$$
\begin{aligned}
T_1^{(0)} &= \frac{m_b - q\cdot v}{2\Delta_0}, \\
T_2^{(0)} &= \frac{m_b}{\Delta_0}, \\
T_3^{(0)} &= \frac{1}{2\Delta_0}, \\
T_4^{(0)} &= 0, \\
T_5^{(0)} &= -\frac{1}{2\Delta_0},
\end{aligned} \tag{2.30}
$$

which reproduce the quark model result when the semileptonic decay rate is calculated using them. As mentioned before, we can use the equation of motion of the heavy quark to eliminate $1/m_b$ corrections. At order $1/m_b^2$ we find the contributions to the form factors

$$
\begin{aligned}
T_1^{(2)} &= \frac{1}{6\Delta_0} m_b (K_B + G_B) + \frac{m_b}{3\Delta_0^2} K_B (3 m_b q\cdot v + 2q^2 - 5 q\cdot v^2) \\
&\quad + \frac{m_b}{3\Delta_0^2} G_B (7 m_b q\cdot v + 2q^2 - 5 q\cdot v^2 - 4m_b^2) \\
&\quad + \frac{4m_b^2}{3\Delta_0^3} K_B (m_b - q\cdot v)(q\cdot v^2 - q^2),
\end{aligned} \tag{2.31}
$$

$$
\begin{aligned}
T_2^{(2)} &= \frac{5m_b}{3\Delta_0} (K_B + G_B) + \frac{14 m_b^2}{3\Delta_0^2} q\cdot v K_B - \frac{2m_b^2}{3\Delta_0^2} (2m_b - 5 q\cdot v) G_B \\
&\quad + \frac{8 m_b^3}{3\Delta_0^3} (q\cdot v^2 - q^2) K_B,
\end{aligned} \tag{2.32}
$$

$$
T_3^{(2)} = \frac{5m_b}{3\Delta_0^2} q\cdot v K_B - \frac{m_b}{3\Delta_0^2} (6m_b - 5 q\cdot v) G_B + \frac{4m_b^2}{3\Delta_0^3} (q\cdot v^2 - q^2) K_B, \tag{2.33}
$$

$$
T_4^{(2)} = \frac{4m_b}{3\Delta_0^2} (K_B + G_B), \tag{2.34}
$$

$$
T_5^{(2)} = -\frac{m_b}{3\Delta_0^2} K_B (4m_b + 5 q\cdot v) - \frac{5m_b}{3\Delta_0^2} q\cdot v G_B + \frac{4m_b^2}{3\Delta_0^3} (q^2 - q\cdot v^2) K_B. \tag{2.35}
$$

Finally, the contributions at third order in the inverse quark mass are given by [9]

$$
\begin{aligned}
T_1^{(3)} &= -\frac{\rho_1 + 3\rho_2}{12\Delta_0 m_b^2} \\
&\quad + \frac{1}{2\Delta_0^2} \left[\rho_1 - \rho_2 + \frac{(\rho_1 + 3\rho_2)\,(q^2 - q\cdot v^2 - m_b^2 + m_b q\cdot v)}{3m_b^2} \right]
\end{aligned} \tag{2.36}
$$

$$
\begin{aligned}
&+\frac{2(\rho_1+3\rho_2)}{3\Delta_0^3 m_b}(m_b-q\cdot v)\left(q^2-q\cdot v^2\right)\\
&-\frac{4\rho_1}{3\Delta_0^4}(m_b-q\cdot v)^2\left(q^2-q\cdot v^2\right),\\
T_2^{(3)} &= \frac{\rho_1+3\rho_2}{6\Delta_0 m_b^2}+\frac{1}{3\Delta_0^2}\left[4\rho_1+6\rho_2-(\rho_1+3\rho_2)\frac{q\cdot v}{m_b}\right] \qquad (2.37)\\
&+\frac{2}{3\Delta_0^3}\left[(4\rho_1+6\rho_2)(m_b-q\cdot v)q\cdot v-3\rho_2 q^2\right]\\
&-\frac{8m_b\rho_1}{3\Delta_0^4}(m_b-q\cdot v)(q^2-q\cdot v^2),\\
T_3^{(3)} &= \frac{\rho_1+3\rho_2}{6m_b^2\Delta_0^2}\,q\cdot v+\frac{2(m_b-q\cdot v)}{3\Delta_0^3}\left[(\rho_1+3\rho_2)\frac{q\cdot v}{m_b}-3\rho_2\right] \qquad (2.38)\\
&-\frac{4\rho_1}{3\Delta_0^4}(m_b-q\cdot v)(q^2-q\cdot v^2),\\
T_4^{(3)} &= \frac{\rho_1+3\rho_2}{3m_b^2\Delta_0^2}-\frac{2\rho_2}{\Delta_0^3}+\frac{4(\rho_1+3\rho_2)}{3m_b\Delta_0^3}\,(m_b-q\cdot v)\,, \qquad (2.39)\\
T_5^{(3)} &= -\frac{\rho_1+3\rho_2}{6m_b^2\Delta_0^2}\,q\cdot v-\frac{2(\rho_1+3\rho_2)}{3m_b\Delta_0^3}\,q\cdot v\,(m_b-q\cdot v)+\frac{2\rho_2 m_b}{\Delta_0^3} \qquad (2.40)\\
&+\frac{4\rho_1}{3\Delta_0^4}(m_b-q\cdot v)(q^2-q\cdot v^2).
\end{aligned}
$$

In order to relate these form factors to the W_i that appear in the differential decay rate, we need to do the integral over the contour C shown in Fig. 2.1. All of the T_i have isolated poles in the $q\cdot v$ plane where $\Delta_0 = m_b^2 - m_c^2 - 2q\cdot v + q^2$ vanishes. The residue at these poles is the imaginary part we are after. One can pick out these imaginary parts by the substitution

$$\frac{1}{\Delta_0^n}\to\frac{(-1)^{n-1}}{(n-1)!}\delta^{(n-1)}(\Delta_0). \qquad (2.41)$$

Here the subscript on the delta function indicates the number of derivatives acting on it. Taking the W_i to be equal to the T_i with this substitution and integrating over the neutrino energy gives a doubly differential decay rate including the nonperturbative corrections up to order $1/m_b^3$. Interesting quantities are the charged lepton spectrum and the hadronic spectrum. The former is obtained by taking the imaginary part of form factors $T_i^{(3)}, i = 1,2,3$ and integrating Eq. (2.17) over q^2 and E_ν. Using the rescaled lepton energy $y = 2E_\ell/m_b$ we find the quark model decay rate and the first

two nonvanishing $1/m_b$ corrections to the lepton spectrum

$$\frac{d\Gamma}{dy} = \frac{d\Gamma^{(0)}}{dy} + \frac{d\Gamma^{(2)}}{dy} + \frac{d\Gamma^{(3)}}{dy}, \tag{2.42}$$

where

$$\frac{d\Gamma^{(0)}}{dy} = \Gamma_0\,\theta(1-r-y)\left[2(3-2y)y^2 - 6y^2r - \frac{6y^2r^2}{(1-y)^2} + \frac{2(3-y)y^2r^3}{(1-y)^3}\right], \tag{2.43}$$

$$\begin{aligned}\frac{d\Gamma^{(2)}}{dy} &= \Gamma_0\left\{K_B\left[-\frac{20y^3}{3} - \frac{4r^2y^3(5-7y+2y^2)}{(1-y)^5} + \frac{8r^3y^3(10-5y+y^2)}{3(1-y)^5}\right]\right. \\ &+ G_B\left[\frac{4y^2(6-5y)}{3} + \frac{8ry^2(3-2y)}{(1-y)^2} + \frac{12r^2y^2(2-y)}{(1-y)^3}\right. \\ &- \left.\left.\frac{20y^2(6-4y+y^2)}{3(1-y)^4}\right]\right\}\theta(1-r-y)\end{aligned} \tag{2.44}$$

and

$$\begin{aligned}\frac{d\Gamma^{(3)}}{dy} &= \frac{\Gamma_0}{m_b^3}\left\{\theta(1-r-y)\left[\frac{8}{3}\left(3\rho_1 + r^2\rho_1 + 9r^2\rho_2 - 3r^3\rho_2\right)\right.\right. \\ &+\frac{8}{3}\rho_1 y(3-2r) - 8\rho_1y^2 - \frac{2}{3}\left(\rho_1+3\rho_2\right)y^3 \\ &-\frac{2\left(4\rho_1+3r^2\rho_1+9r^2\rho_2\right)}{1-y} - \frac{2r\left(8\rho_1+9r\rho_1+27r\rho_2\right)}{3(1-y)^2} \\ &+\frac{2r\left(8\rho_1+17r\rho_1+4r^2\rho_1-9r\rho_2+12r^2\rho_2\right)}{3(1-y)^3} \\ &+\frac{2r^2\left(3\rho_1+4r\rho_1+9\rho_2+12r\rho_2\right)}{(1-y)^4} - \frac{8r^2\left(\rho_1+3r\rho_1+3r\rho_2\right)}{(1-y)^5} \\ &\left.\left.+\frac{40r^3\rho_1}{3(1-y)^6}\right] - \delta(1-r-y)\frac{2(1-r)^4(1+r)^2\rho_1}{3r^2}\right\}.\end{aligned} \tag{2.45}$$

Here we defined $r = (m_c/m_b)^2$. Note the contribution from the δ-function at the endpoint of the lepton spectrum. For $b \to u$ transition such singular terms in the lepton spectrum appear already at order $1/m_b^2$, but for $b \to c$ they do not appear until order $1/m_b^3$. This is easily explained if one recalls that the most singular contributions to the lepton spectrum at a given order $1/m_b^n$ can be obtained from the spectator

model result by the "averaging" procedure of Ref.[3], which involves differentiating n times with respect to y. For a massless final state quark the spectator model spectrum has the form $f(y)\theta(1-y)$ with $f(1) \neq 0$, and thus differentiation produces the $n-1$-st derivative of the δ-function $\delta^{(n-1)}(1-y)$. For a massive quark in the final state the spectator model spectrum and its first derivative vanish at the end point $y = 1 - r$. Hence at order $1/m_b^n$ the most singular contribution is proportional to $\delta^{(n-3)}(1-y-r)$.

2.3 The hadronic invariant mass spectrum

A second differential rate that can be used to obtain information on the HQET parameters $\bar{\Lambda}$ and λ_1 is the hadronic invariant mass spectrum. As before, we present the complete expression for this differential rate, expressing the $1/m_b^2$ contributions in terms of K_b and G_b, which have an implicit mass dependence. To obtain an expression for the hadronic invariant mass spectrum, we integrate Eq. (2.17) over E_ν and express the result in terms of rescaled hadronic variables $\hat{E}_0 = (m_b - q\cdot v)/m_b$ and $\hat{s}_0 = (m_b^2 - 2q\cdot v + q^2)/m_b^2$, which are the energy and the square of the invariant mass of the hadronic final state, respectively. This results in an expression of the form

$$\frac{d\Gamma}{d\hat{s}_0 d\hat{E}_0} = \frac{d\Gamma^{(0)}}{d\hat{s}_0 d\hat{E}_0} + \frac{d\Gamma^{(2)}}{d\hat{s}_0 d\hat{E}_0} + \frac{d\Gamma^{(3)}}{d\hat{s}_0 d\hat{E}_0}, \tag{2.46}$$

where

$$\begin{aligned}\frac{d\Gamma^{(0)}}{d\hat{s}_0 d\hat{E}_0} &= 32\Gamma_0\theta(\hat{E}_0 - \sqrt{\hat{s}_0})\theta(1+\hat{s}_0-2\hat{E}_0)\sqrt{\hat{E}_0^2-\hat{s}_0}\,\delta(\hat{s}_0 - r)\times \\ &\quad \left[\left(1-2\hat{E}_0+\hat{s}_0\right)\frac{3\hat{E}_0}{2} + \hat{E}_0^2 - \hat{s}_0\right],\end{aligned} \tag{2.47}$$

$$\begin{aligned}\frac{d\Gamma^{(2)}}{d\hat{s}_0 d\hat{E}_0} &= 32\Gamma_0\theta(\hat{E}_0 - \sqrt{\hat{s}_0})\theta(1+\hat{s}_0-2\hat{E}_0)\sqrt{\hat{E}_0^2-\hat{s}_0}\times \\ &\quad \left\{\delta(\hat{s}_0 - r)(K_B + G_B)\left[\frac{1}{2}(1-2\hat{E}_0+\hat{s}_0) + \frac{5}{3}(\hat{E}_0^2-\hat{s}_0)\right]\right.\end{aligned} \tag{2.48}$$

$$
\begin{aligned}
&+\ \delta'(\hat{s}_0 - r)\Big[(1 - 2\hat{E}_0 + \hat{s}_0)\Big(K_B(5\hat{E}_0^2 - 3\hat{E}_0 - 2\hat{s}_0) + G_B(5\hat{E}_0^2 + \hat{E}_0 - 2\hat{s}_0)\Big) \\
&+\ (\hat{E}_0^2 - \hat{s}_0)\Big(\frac{14}{3}K_B(\hat{E}_0 - 1) + \frac{2}{3}G_B(5\hat{E}_0 - 3)\Big)\Big] \\
&+\ \delta''(\hat{s}_0 - r)K_B(\hat{E}_0^2 - \hat{s}_0)\Big[2(1 - 2\hat{E}_0 + \hat{s}_0)\hat{E}_0 + \frac{4}{3}(\hat{E}_0^2 - \hat{s}_0)\Big]\Big\},
\end{aligned}
$$

and

$$
\begin{aligned}
\frac{d\Gamma^{(3)}}{d\hat{s}_0 d\hat{E}_0} &= \frac{8\Gamma_0}{3m_b^3}\Theta(\hat{E}_0 - \sqrt{\hat{s}_0})\Theta(1 + \hat{s}_0 - 2\hat{E}_0)\sqrt{\hat{E}_0^2 - \hat{s}_0}\,\times \qquad (2.49)\\
&\Big\{(\rho_1 + 3\rho_2)(-3 + 6\hat{E}_0 + 2\hat{E}_0^2 - 5\hat{s}_0)\delta(\hat{s}_0 - r) - 2\Big[9(\rho_1 - \rho_2) \\
&+\ 6(\rho_1 - \rho_2)\hat{s}_0 + 3(\rho_1 + 3\rho_2)\hat{s}_0^2 - (3(7\rho_1 - 3\rho_2) + 11(\rho_1 + 3\rho_2)\hat{s}_0)\hat{E}_0 \\
&+\ 3((3\rho_1 + 5\rho_2) - (\rho_1 + 3\rho_2)\hat{s}_0)\hat{E}_0^2 + 8(\rho_1 + 3\rho_2)\hat{E}_0^3\Big]\delta'(\hat{s}_0 - r) \\
&-\ 4(\hat{E}_0^2 - \hat{s}_0)\Big[3(1 + \hat{s}_0)\rho_2 - (1 - 3\hat{s}_0)(\rho_1 + 3\rho_2)\hat{E}_0 - 2(\rho_1 + 6\rho_2)\hat{E}_0^2\Big]\delta''(\hat{s}_0 - r) \\
&+\ \frac{8}{3}\hat{E}_0(\hat{E}_0^2 - \hat{s}_0)\rho_1\Big[2\hat{s}_0 - 3(1 + \hat{s}_0)\hat{E}_0 + 4\hat{E}_0^2\Big]\delta'''(\hat{s}_0 - r)\Big\}.
\end{aligned}
$$

Applications of these expressions will be discussed in Chapter 4.

2.4 The expansion of the states

Above we computed the $1/m_b^3$ corrections to the inclusive differential B decay rate from the local dimension-six operators in the OPE. However, there are other sources of $1/m_b^3$ corrections. At order $1/m_b^2$ the OPE yields the decay rate in terms of the two matrix elements

$$
\begin{aligned}
&\langle B(v)\,|\bar{h}_v\,(iD_\perp)^2\,h_v|\,B(v)\rangle, \qquad (2.50)\\
&\tfrac{1}{3}\langle B(v)\,|\bar{h}_v\,\tfrac{g}{2}\,\sigma_{\mu\nu}\,G^{\mu\nu}\,h_v|\,B(v)\rangle \quad ,
\end{aligned}
$$

where $|B(v)\rangle$ is the physical B-meson state, rather than the state of the effective theory in the infinite mass limit $|B_\infty(v)\rangle$. Thus these matrix elements are mass-dependent. At order $1/m_b^2$ this distinction is irrelevant, but at higher orders this mass dependence has to be taken into account explicitly. We express the physical

states through the states in the infinite mass limit of HQET using the Gell-Mann and Low theorem (see, e.g., Ref. [15]). This theorem implies that, to first order in $1/m_b$, $|B(v)\rangle$ is given by

$$|\,B(v)\rangle = \left[1 + i\int d^3x \int_{-\infty}^{0} dt\mathcal{L}_I(x) - \frac{1}{V}\langle B_\infty(v)\,|i\int d^3x\int_{-\infty}^{0} dt\mathcal{L}_I(x)|\,B_\infty(v)\rangle\right]|\,B_\infty(v)\rangle, \tag{2.51}$$

where V is the normalization volume and

$$\mathcal{L}_I = \frac{1}{2m_b}\bar{h}_v\,(iD_\perp)^2\,h_v + \frac{1}{2m_b}\bar{h}_v\,\frac{g}{2}\,\sigma_{\mu\nu}\,G^{\mu\nu}\,h_v. \tag{2.52}$$

Using Eq. (2.51), one can easily expand the matrix elements in Eq. (2.50) to order $1/m_b^3$. It is convenient to introduce the following notation:

$$\begin{aligned}
\langle H_\infty(v)|\bar{h}_v\,(iD_\perp)^2\,h_v i\int d^3x\int_{-\infty}^{0} dt\mathcal{L}_I(x)|H_\infty(v)\rangle + h.c. &= \frac{\mathcal{T}_1 + d_H\mathcal{T}_2}{m_b}, \\
\langle H_\infty(v)|\bar{h}_v\,\frac{g}{2}\,\sigma_{\mu\nu}\,G^{\mu\nu}\,h_v i\int d^3x\int_{-\infty}^{0} dt\mathcal{L}_I(x)|H_\infty(v)\rangle + h.c. &= \frac{\mathcal{T}_3 + d_H\mathcal{T}_4}{m_b}
\end{aligned} \tag{2.53}$$

for the matrix elements of these nonlocal operators. We then find

$$\begin{aligned}
\langle B(v)\,|\bar{h}_v\,(iD_\perp)^2\,h_v|\,B(v)\rangle &= \lambda_1 + \frac{\mathcal{T}_1 + 3\mathcal{T}_2}{m_b}, \\
\frac{1}{3}\langle B(v)\,|\bar{h}_v\,\frac{g}{2}\,\sigma_{\mu\nu}\,G^{\mu\nu}\,h_v|\,B(v)\rangle &= \lambda_2 + \frac{\mathcal{T}_3 + 3\mathcal{T}_4}{3m_b}.
\end{aligned} \tag{2.54}$$

Thus these order $1/m_b^3$ corrections to the inclusive $B \to X_c\ell\bar{\nu}$ decay rate are parametrized by the matrix elements $\mathcal{T}_1 - \mathcal{T}_4$ of four nonlocal operators. These matrix elements are related to those introduced in Ref. [12]: $\mathcal{T}_1 = \rho_{\pi\pi}^3, \mathcal{T}_2 = \frac{1}{6}\rho_{\pi G}^3, \mathcal{T}_3 = \rho_S^3, \mathcal{T}_4 = \frac{1}{3}\rho_A^3 + \frac{1}{6}\rho_{\pi G}^3$.

This class of $1/m_b^3$ corrections can be included in any quantity known at order $1/m_b^2$ by using Eq. (2.54) to evaluate the matrix elements of the dimension-five operators. In particular the corrections to the form factors and the differential rates in the previous section and Ref. [3] can be obtained in this way.

2.5 The meson masses

For comparison with experiments it is necessary to express the pole quark masses m_c and m_b in terms of HQET matrix elements and physical observables, e.g., the spin averaged meson masses $\overline{m}_B$ and $\overline{m}_D$, where $\overline{m}_{Meson} = (m_P + 3m_V)/4$. For this purpose one needs to know how quark masses are related to hadron masses at order $1/m_b^3$. Our starting point is the identity

$$m_H = \frac{V}{2}\frac{\langle H_\infty(v)\,|\mathcal{H}|\,H(v)\rangle}{\langle H_\infty(v)\,|\,H(v)\rangle} + h.c.\,, \tag{2.55}$$

where V is the normalization volume and $\mathcal{H}$ is the full Hamiltonian density including light degrees of freedom[1]. This equation holds in the rest frame of the hadron. Then we split $\mathcal{H}$ into the leading term and the terms suppressed by powers of $1/m_b$, $\mathcal{H} = \mathcal{H}_0 + \mathcal{H}_1$, and use the fact that $|\,H_\infty(v)\rangle$ is an eigenstate of $\int d^3x\mathcal{H}_0$ with eigenvalue $m_b + \bar{\Lambda}$. The use of the Foldy-Wouthuysen-transformed fields, Eq. (2.22), ensures that there is no implicit dependence on m_b in h_v. Also, there are no time-derivatives in the HQET Lagrangian beyond leading order, as can be seen, e.g., from Eq. (82) of Ref. [5]. Therefore, we have $\mathcal{H}_1 = -\mathcal{L}_1$. Using the Gell-Mann and Low theorem, the general expression for the hadron mass reads

$$m_H = m_b + \bar{\Lambda} - \frac{V}{2}\left[\frac{\langle H_\infty(v)\,|\mathcal{L}_1\,T\exp\left(i\int d^3x\int_{-\infty}^0 dt\mathcal{L}_1(x)\right)|\,H_\infty(v)\rangle}{\langle H_\infty(v)\,|T\exp\left(i\int d^3x\int_{-\infty}^0 dt\mathcal{L}_1(x)\right)|\,H_\infty(v)\rangle} + h.c.\right]. \tag{2.56}$$

Expanding Eq. (2.56) to order $1/m_b^3$, we obtain the mass formula:

$$\begin{aligned} m_H &= m_b + \bar{\Lambda} - \langle H_\infty(v)\,|\mathcal{L}_I + \mathcal{L}_{II}|\,H_\infty(v)\rangle \\ &\quad - \left[\frac{1}{2}\langle H_\infty(v)\,|\mathcal{L}_I i\int d^3x\int_{-\infty}^0 dt\mathcal{L}_I(x)|\,H_\infty(v)\rangle + h.c.\right], \end{aligned} \tag{2.57}$$

[1] If one starts from a similar identity with eigenstates of $\mathcal{H}$ on both sides of the matrix element, one obtains the same result after a somewhat more cumbersome calculation.

where [5]

$$\mathcal{L}_{II} = -\frac{1}{4m_b^2}\bar{h}_v\, i\not{D}_\perp (iv\cdot D) i\not{D}_\perp\, h_v + \frac{1}{8m_b^2}\bar{h}_v\, (i\not{D}_\perp)^2 (iv\cdot D)\, h_v + \frac{1}{8m_b^2}\bar{h}_v\, (iv\cdot D)(i\not{D}_\perp)^2\, h_v, \tag{2.58}$$

and $\mathcal{L}_I$ is given in Eq. (2.52). Eq. (2.57) contains expectation values of both local and nonlocal operators. The local part can be evaluated in terms of the matrix elements $\lambda_1, \lambda_2, \rho_1$ and ρ_2, while the nonlocal matrix elements can be expressed through $\mathcal{T}_1 - \mathcal{T}_4$ defined in Eqs. (2.53). In terms of these matrix elements the meson mass is given by

$$m_H = m_b + \bar{\Lambda} - \frac{\lambda_1 + d_H\lambda_2}{2m_b} + \frac{\rho_1 + d_H\rho_2}{4m_b^2} - \frac{\mathcal{T}_1 + \mathcal{T}_3 + d_H(\mathcal{T}_2 + \mathcal{T}_4)}{4m_b^2}, \tag{2.59}$$

in agreement with Refs. [5, 12].

The differential and total decay rates are functions of the ratio of quark masses which can be expressed in terms of the spin averaged meson masses

$$\begin{aligned}\frac{m_c}{m_b} &= \frac{\overline{m}_D}{\overline{m}_B} - \frac{\bar{\Lambda}}{\overline{m}_B}\left(1 - \frac{\overline{m}_D}{\overline{m}_B}\right) + \frac{\lambda_1}{2\overline{m}_B^2}\left(\frac{\overline{m}_B}{\overline{m}_D} - \frac{\overline{m}_D}{\overline{m}_B}\right) - \frac{\bar{\Lambda}^2}{\overline{m}_B^2}\left(1 - \frac{\overline{m}_D}{\overline{m}_B}\right) \\ &- \frac{\bar{\Lambda}^3}{\overline{m}_B^3}\left(1 - \frac{\overline{m}_D}{\overline{m}_B}\right) + \frac{\bar{\Lambda}\lambda_1}{2\overline{m}_B^3}\left(1 + \frac{\overline{m}_B}{\overline{m}_D} - 3\frac{\overline{m}_D}{\overline{m}_B} + \frac{\overline{m}_B^2}{\overline{m}_D^2}\right) - \frac{\rho_1 - \mathcal{T}_1 - \mathcal{T}_3}{4\overline{m}_B^3}\left(\frac{\overline{m}_B^2}{\overline{m}_D^2} - \frac{\overline{m}_D}{\overline{m}_B}\right),\end{aligned} \tag{2.60}$$

where $\overline{m}_D$ and $\overline{m}_B$ are defined as $\overline{m}_{Meson} = (m_P + 3m_V)/4$.

The familiar relation of the HQET matrix element λ_2 to the mass splitting between B and B^* mesons also needs to be extended to include the $1/m_b^3$ contributions. Using Eq. (2.59) to express the quark mass through the meson mass and $\bar{\Lambda}$, we find

$$m_{H^*} - m_H = \Delta m_H = 2\frac{\kappa(m_Q)\lambda_2(m_b)}{m_H}\Big(1 + \frac{\bar{\Lambda}}{m_H}\Big) - \frac{\rho_2}{m_H^2} + \frac{\mathcal{T}_2 + \mathcal{T}_4}{m_H^2}, \tag{2.61}$$

where $\kappa(m_Q) = (\alpha_s(m_Q)/\alpha_s(m_b))^{3/\beta_0}$ takes account of the scale dependence of λ_2. We can use the $B - B^*$ and $D - D^*$ mass splitting to extract the numerical value of some of the HQET matrix elements:

$$\lambda_2(m_b) = \frac{\Delta m_B m_B^2 - \Delta m_D m_D^2}{2(m_B - \kappa(m_c)m_D)},$$

$$\rho_2 - \mathcal{T}_2 - \mathcal{T}_4 = \frac{\kappa(m_c) m_B^2 \Delta m_B (m_D + \bar{\Lambda}) - m_D^2 \Delta m_D (m_B + \bar{\Lambda})}{m_B + \bar{\Lambda} - \kappa(m_c)(m_D + \bar{\Lambda})}. \quad (2.62)$$

2.6 The total decay rate

The total rate is given by integrating Eq. (2.42) or Eq. (2.46) over the remaining variables:

$$\Gamma = \Gamma^{(0)} + \Gamma^{(2)} + \Gamma^{(3)}, \quad (2.63)$$

where

$$\Gamma^{(0)} = \Gamma_0 \left[1 - 8r + 8r^3 - r^4 - 12r^2 \log r\right], \quad (2.64)$$

$$\begin{aligned} \Gamma^{(2)} = \Gamma_0 \Big[& K_B(-1 + 8r - 8r^3 + r^4 + 12r^2 \log r) \\ & + G_B(3 - 8r + 24r^2 - 24r^3 + 5r^4 + 12r^2 \log r)\Big], \end{aligned} \quad (2.65)$$

and

$$\begin{aligned} \Gamma^{(3)} = \frac{\Gamma_0}{6m_b^3}[\rho_1 & (77 - 88r + 24r^2 - 8r^3 - 5r^4 + 48 \log r + 36r^2 \log r) \\ & + \rho_2(27 - 72r + 216r^2 - 216r^3 + 45r^4 + 108r^2 \log r)]. \end{aligned} \quad (2.66)$$

The part of Eq. (2.66) that diverges logarithmically as $r \to 0$ agrees with the corresponding expression in Ref. [16]. There is nothing wrong with the logarithmic divergence, since our calculation is valid only for the charm mass significantly larger than Λ_{QCD}. It is the latter condition that allowed us to discard the diagram in Fig. 2.2b. For a discussion of the corrections to the total semileptonic decay rate from dimension-six operators with a light quark in the final state, see Ref. [16].

To compare the expressions for the total rate with experimental measurements, K_b, G_b should be expressed in terms of $\lambda_{1,2}$, and Eq. (2.60) should be used to rewrite the ratio of quark masses in terms of the meson masses. Once the values of the HQET matrix elements are known, this provides a theoretical prediction for the total semileptonic decay width of the B meson. The results in this chapter show that the

nonperturbative corrections to the semileptonic B-decay affect both the normalization of the total rate and the shape of the differential rates. In Chapter 4 we will see that one can define observables that are sensitive to the shape of the spectra and extract the HQET matrix elements from the comparison to experimental data. The $1/m_b^3$ corrections we computed here will be useful for estimating the theoretical uncertainties in this extraction.

Chapter 3 Perturbative corrections to the lepton spectrum in $B \to X_c \ell \nu$

3.1 Introduction

The electron spectrum in semileptonic inclusive $B \to X_c \ell \bar{\nu}_\ell$ decays receives both perturbative and nonperturbative corrections. Knowledge of the shape of the spectrum can provide insights into nonperturbative effects in B meson decays, and thereby also give some information on the weak mixing angle $|V_{cb}|$. In the previous chapter we have shown that in the framework of Heavy Quark Effective Theory that the quark level decay rate is the first term in a power series expansion in the small parameter Λ_{QCD}/m_b [11]. For infinitely heavy quarks the free quark model is an exact description of heavy meson physics. At finite quark masses the first few terms in the heavy quark expansion have to be taken into account. Expressions for these nonperturbative corrections to the lepton spectrum are known to order $(\Lambda_{QCD}/m_b)^3$ [3, 4, 14, 16, 9] and the $\mathcal{O}(\alpha_s)$ perturbative corrections to the free quark decay were given in [17].

The dominant remaining uncertainties are the two-loop corrections to the quark level decay rate and the perturbative corrections to the coefficients of the HQET matrix elements in the operator product expansion. Here we examine the former. This is equivalent to calculating the Wilson coefficient of the leading operator in the OPE. While a full two-loop calculation of the electron spectrum is a rather daunting task, it is possible to calculate the piece of the two-loop correction that is proportional to $\beta_0 = 11 - 2/3 n_f$ with relative ease by computing the one-loop QCD corrections with a massive gluon. The $\alpha_s^2 \beta_0$ parts of the two-loop correction may then be obtained from a dispersion integral over the gluon mass [18]. If there are no gluons in the tree level graph, the $\alpha_s^2 \beta_0$ part of the two-loop contribution is believed to dominate the full α_s^2 result because β_0 is rather large. Several examples supporting this belief are

listed in [19], while one counterexample can be found in [20].

A recent calculation [19] of the $\alpha_s^2\beta_0$ correction to the total inclusive rate for $B \to X_c\ell\bar{\nu}_\ell$ decays showed that the $\alpha_s^2\beta_0$ parts of the two-loop correction are approximately half as big as the one-loop contribution, resulting in a rather low BLM scale [21] of $\mu_{BLM} = 0.13 m_b$. For the electron spectrum we find that this part of the second order correction also amounts to about 50% of the order α_s contribution, at all electron energies except those close to the endpoint. Close to the endpoint the corrections are roughly equal in magnitude.

In following two sections we give analytic expressions for the contributions from virtual and real gluon radiation. The last phase space integral in the virtual correction and the last two integrals in the bremsstrahlung are done numerically. In Sect. 3.4 we combine the results from the previous two sections to obtain the $\alpha_s^2\beta_0$ corrections to the electron spectrum. The remaining two sections we give the explicit expressions for the the scalar two and three-point functions that occur in the expressions for the virtual corrections and provide an interpolating polynomial which reproduces the two-loop correction calculated here.

3.2 Virtual corrections

The corrections from massive virtual gluons can be calculated in complete analogy to the usual one-loop QCD corrections. The ultraviolet divergence in the vertex correction cancels when combined with the quark wave function renormalizations. There is no infrared divergence since we do the calculation with a massive gluon. The virtual one-loop correction to the differential rate can be written as

$$\begin{aligned}\frac{d\Gamma^{(1)}_{virt}(\hat{\mu})}{dy} &= \alpha_s^{(V)} \frac{|V_{cb}|^2 G_F^2 m_b^5}{48\pi^4} \int d\hat{q}^2 \Big[2(y-\hat{q}^2)(\hat{q}^2+1-r^2-y)(a_1+a_{wr}) - 2r\hat{q}^2 a_2 \\ &\quad + (\hat{q}^2(y-1)+y(1-r^2)-y^2)a_3 \Big] \end{aligned} \tag{3.1}$$

where $\hat{\mu} = \mu/m_b$ is the rescaled gluon mass, and $y = 2E_e/m_b$, $r = m_c/m_b$, and $\hat{q}^2 = q^2/m_b^2$ are the rescaled electron energy, charm mass, and momentum transfer,

respectively. The limits for the integration over $\hat{q}^2$ are

$$0 \leq \hat{q}^2 \leq \frac{y(1-y-r^2)}{1-y}, \qquad 0 \leq y \leq 1-r^2. \tag{3.2}$$

The functions $a_{wr}(\hat{q}^2)$ and $a_i(\hat{q}^2)$, $i = 1, 2, 3$ are the contributions from the wave function renormalization and the vertex correction respectively. They can be expressed in terms of the scalar two- and three-point functions B_0 and C_0 [22], and the derivative $B_0' = \partial B_0(a,b,c)/\partial a$. Explicit expressions for these functions are given in Section 3.5. Using the standard decomposition for the vector and tensor loop integrals [22], we obtain

$$\begin{aligned}
a_1 &= -2 + 4C_{00} + 2(C_{11} + C_1 + r^2 C_{22} + r^2 C_2) \\
&\quad +2(1 - \hat{q}^2 + r^2)(C_{12} + C_0 + C_1 + C_2), \\
a_2 &= 2r(C_1 + C_2), \\
a_3 &= -4(C_{11} + C_{12} + C_1) - 4r^2(C_{12} + C_{22} + C_2), \\
a_{wr} &= \frac{1}{2}\Big[2 - B_0(1,\hat{\mu}^2,1) - B_0(r^2,\hat{\mu}^2,r^2) \\
&\quad +(1-\hat{\mu}^2)\Big(B_0(1,\hat{\mu}^2,1) - B_0(0,\hat{\mu}^2,1)\Big) \\
&\quad +\frac{(r^2-\hat{\mu}^2)}{r^2}\Big(B_0(r^2,\hat{\mu}^2,r^2) - B_0(0,\hat{\mu}^2,r^2)\Big) \\
&\quad +2(2+\hat{\mu}^2)B_0'(1,\hat{\mu}^2,1) \\
&\quad +2(2r^2+\hat{\mu}^2)B_0'(r^2,\hat{\mu}^2,r^2)\Big].
\end{aligned} \tag{3.3}$$

Defining $f_1 = 1 + r^2 - \hat{q}^2$ and $f_2 = (f_1^2 - 4r^2)$, the coefficient functions take the form

$$\begin{aligned}
C_{00} &= \frac{1}{4f_2}\Big[f_2 + \hat{\mu}^2(f_1-2)B_0(1,1,\hat{\mu}^2) + \hat{\mu}^2(f_1-2r^2)B_0(r^2,r^2,\hat{\mu}^2) \\
&\quad +(f_2 + 2\hat{q}^2\hat{\mu}^2)B_0(\hat{q}^2,1,r^2) + 2\hat{\mu}^2(f_2 + \hat{q}^2\hat{\mu}^2)C_0(1,\hat{q}^2,r^2,\hat{\mu}^2,1,r^2)\Big],
\end{aligned} \tag{3.4}$$

$$\begin{aligned}
C_{11} &= \frac{r^2}{f_2} + \frac{(f_1-2r^2)(1-r^2)}{2\hat{q}^2 f_2}B_0(0,1,r^2) + \frac{f_1(\hat{\mu}^2-1)}{2f_2}B_0(0,1,\hat{\mu}^2) \\
&\quad +\frac{3r^2\hat{\mu}^2(f_1-2r^2)}{f_2^2}B_0(r^2,r^2,\hat{\mu}^2)
\end{aligned} \tag{3.5}$$

$$
\begin{aligned}
&+\frac{2\hat{q}^2\hat{\mu}^2(f_2+6\hat{q}^2r^2)-f_2(f_2+2\hat{q}^2r^2)}{2\hat{q}^2f_2^2}B_0(\hat{q}^2,1,r^2)\\
&+\frac{\hat{\mu}^2\Big(6r^2(f_1-2)-f_2(f_1+2)\Big)}{2f_2^2}B_0(1,1,\hat{\mu}^2)\\
&+\frac{2\hat{\mu}^2r^2f_2+\hat{\mu}^4(f_2+6\hat{q}^2r^2)}{f_2^2}C_0(1,\hat{q}^2,r^2,\hat{\mu}^2,1,r^2),\\
C_{22} &= \frac{1}{f_2}+\frac{(1-r^2)(2-f_1)}{2\hat{q}^2f_2}B_0(0,1,r^2)\\
&+\frac{2\hat{q}^2\hat{\mu}^2(f_2+6\hat{q}^2)-f_2(f_2+2\hat{q}^2)}{2\hat{q}^2f_2^2}B_0(\hat{q}^2,1,r^2)\\
&+\frac{(\hat{\mu}^2-r^2)f_1}{2r^2f_2}B_0(0,r^2,\hat{\mu}^2)+\frac{3\hat{\mu}^2(f_1-2)}{f_2^2}B_0(1,1,\hat{\mu}^2) \qquad (3.6)\\
&+\frac{\hat{\mu}^2\Big(6r^2(f_1-2r^2)-f_2(f_1+2r^2)\Big)}{2r^2f_2^2}B_0(r^2,r^2,\hat{\mu}^2)\\
&+\frac{\hat{\mu}^2\Big(2f_2+\hat{\mu}^2(f_2+6\hat{q}^2)\Big)}{f_2^2}C_0(1,\hat{q}^2,r^2,\hat{\mu}^2,1,r^2),\\
C_{12} &= \frac{-f_1}{2f_2}+\frac{(1-r^2)(2r^2-f_1)}{2\hat{q}^2f_2}B_0(0,1,r^2)+\frac{r^2-\hat{\mu}^2}{f_2}B_0(0,r^2,\hat{\mu}^2)\\
&+\frac{\hat{\mu}^2\Big(6(f_1-2r^2)-f_2\Big)}{2f_2^2}B_0(1,1,\hat{\mu}^2)\\
&+\frac{\hat{\mu}^2\Big(6r^2(f_1-2)-f_2\Big)}{2f_2^2}B_0(r^2,r^2,\hat{\mu}^2) \qquad (3.7)\\
&+\frac{f_2(f_2+\hat{q}^2f_1)-2\hat{\mu}^2\hat{q}^2(3\hat{q}^2f_1+f_2)}{2\hat{q}^2f_2^2}B_0(\hat{q}^2,1,r^2)\\
&+\frac{\hat{\mu}^2\Big(-f_1f_2-\hat{\mu}^2(3\hat{q}^2f_1+f_2)\Big)}{f_2^2}C_0(1,\hat{q}^2,r^2,\hat{\mu}^2,1,r^2),\\
C_1 &= \frac{1}{f_2}\Big[f_1B_0(1,1,\hat{\mu}^2)+(2r^2-f_1)B_0(\hat{q}^2,1,r^2)-2r^2B_0(r^2,r^2,\hat{\mu}^2)\\
&+\hat{\mu}^2(2r^2-f_1)C_0(1,\hat{q}^2,r^2,\hat{\mu}^2,1,r^2)\Big], \qquad (3.8)\\
C_2 &= \frac{1}{f_2}\Big[-2B_0(1,1,\hat{\mu}^2)+(2-f_1)B_0(\hat{q}^2,1,r^2)+f_1B_0(r^2,r^2,\hat{\mu}^2)\\
&+\hat{\mu}^2(2-f_1)C_0(1,\hat{q}^2,r^2,\hat{\mu}^2,1,r^2)\Big]. \qquad (3.9)
\end{aligned}
$$

The infinite parts of the regularized two-point functions can be shown to cancel in Eq. (3.1). In the limit $\hat{\mu}\to 0$ the vertex correction diverges logarithmically.

This divergence will be canceled by corresponding divergences in the bremsstrahlung contributions discussed in the next section.

3.3 Bremsstrahlung

The bremsstrahlung correction is found in the usual manner, by inserting a real gluon on the c and b quark lines. The calculation here is complicated by the four-body phase space with two massive final states. We follow the standard procedure of decomposing the four-body phase space into a two- and a three-body phase space by introducing the four-momentum $P = p_c + p_g$. In the rest frame of the b quark this decomposition reads

$$dR_4 = dP^2 \; dR_3(m_b; p_e, p_{\bar{\nu}}, P) dR_2(P; p_c, p_g). \tag{3.10}$$

The $\mathcal{O}(\alpha_s)$ bremsstrahlung correction to the differential rate is given in terms of dimensionless variables ($\hat{P}^0 = P^0/m_b$, $\hat{P}^2 = P^2/m_b^2$) by

$$\begin{aligned}
\frac{d\Gamma^{(1)}_{brems}(\hat{\mu})}{dy} &= \alpha_s^{(V)} \frac{G_F^2 \, |V_{cb}|^2 \, m_b^5}{192 \, \pi^4} \int d\hat{P}^2 \; d\hat{P}^0 \; (\hat{P^0}^2 - \hat{P}^2)^{-5/2} \\
&\times \Big[2b_1(1 - 2\hat{P}^0 + \hat{P}^2) + b_2(2 - 2\hat{P}^0 - y)y \\
&+ b_3(1 - y - \hat{P}^2)(2\hat{P}^0 + y - \hat{P}^2 - 1) \\
&+ b_4(1 - y - \hat{P}^2)y \\
&+ b_5(2\hat{P}^0 + y - 2)(1 - 2\hat{P}^0 - y + \hat{P}^2) \Big].
\end{aligned} \tag{3.11}$$

For convenience the above rate has been written in terms of the coefficients b_i

$$b_1 = (\hat{P^0}^2 - \hat{P}^2) \left(\hat{P}^2(c_2 - c_1) + \hat{P^0}^2 c_1 + c_3 - \hat{P}^0(c_4 + c_5) \right), \tag{3.12}$$

$$b_2 = (\hat{P^0}^2 - \hat{P}^2)\hat{P}^2 c_1 + 3\hat{P}^4 c_2 + (\hat{P}^2 + 2\hat{P^0}^2)c_3 - 3\hat{P}^0\hat{P}^2(c_4 + c_5), \tag{3.13}$$

$$b_3 = (\hat{P^0}^2 - \hat{P}^2)c_1 + (\hat{P}^2 + 2\hat{P}^0)c_2 + 3c_3 - 3\hat{P}^0(c_4 + c_5), \tag{3.14}$$

$$b_4 = -\hat{P}^0(\hat{P^0}^2 - \hat{P}^2)c_1 - 3\hat{P}^0\hat{P}^2 c_2 - 3\hat{P}^0 c_3 + (\hat{P^0}^2 + 2\hat{P}^2)c_4 + 3\hat{P^0}^2 c_5, \tag{3.15}$$

$$b_5 = -\hat{P}^0(\hat{P^0}^2 - \hat{P}^2)c_1 - 3\hat{P}^0\hat{P}^2 c_2 - 3\hat{P}^0 c_3 + 3\hat{P^0}^2 c_4 + (\hat{P^0}^2 + 2\hat{P}^2)c_5, \tag{3.16}$$

which are linear combinations of

$$
\begin{aligned}
c_1 &= \frac{4(v_+^2 - v_-^2)}{h} \\
&\quad + \frac{2[(h+\hat{\mu}^2 - 2\hat{P^0})^2 + (\hat{\mu}^2 - 2\hat{P^0})^2 + 2\hat{\mu}^2(1+r^2)]}{h} \ln(\frac{2v_+ - \hat{\mu}^2}{2v_- - \hat{\mu}^2}) \\
&\quad + \frac{4(2+\hat{\mu}^2)(h - 2\hat{P^0})(v_+ - v_-)}{(2v_+ - \hat{\mu}^2)(2v_- - \hat{\mu}^2)} - \frac{8[(z+\hat{\mu}^2)(\hat{P^0} - h) + z\hat{P^0}](v_+ - v_-)}{h^2}, \qquad (3.17) \\
c_2 &= \frac{2(v_+^2 - v_-^2)(2-h)}{h} \\
&\quad - \frac{[h\hat{\mu}^2(3\hat{\mu}^2 - 4\hat{P^0}) + 4\hat{\mu}^2(2\hat{P^0} - 1) - 16\hat{P^0}^2]}{h} \ln(\frac{2v_+ - \hat{\mu}^2}{2v_- - \hat{\mu}^2}) \\
&\quad + \frac{2(\hat{\mu}^4 - 4)(2\hat{P^0} - \hat{\mu}^2)(v_+ - v_-)}{(2v_+ - \hat{\mu}^2)(2v_- - \hat{\mu}^2)} \qquad (3.18) \\
&\quad - \frac{4[h^2(\hat{\mu}^2 - \hat{P^0}) + 2\hat{P^0}(\hat{\mu}^2 + 2\hat{P^2})](v_+ - v_-)}{h^2}, \\
c_3 &= \frac{[(\hat{P^2} + r^2)(h^2 + 2(\hat{\mu}^2 - 2\hat{P^0})(h - 2\hat{P^0})) - h\hat{\mu}^4 + 4r^2\hat{P^2}\hat{\mu}^2]}{h} \ln(\frac{2v_+ - \hat{\mu}^2}{2v_- - \hat{\mu}^2}) \\
&\quad + \frac{2(2+\hat{\mu}^2)(\hat{\mu}^2 - r^2 - \hat{P^2})(2\hat{P^0} - \hat{\mu}^2 - h)(v_+ - v_-)}{(2v_+ - \hat{\mu}^2)(2v_- - \hat{\mu}^2)} \\
&\quad - \frac{4[(\hat{P^2} + r^2)(h\hat{P^0} - hz + \hat{\mu}^2\hat{P^0}) + 4r^2\hat{P^2}\hat{P^0}](v_+ - v_-)}{h^2}, \qquad (3.19) \\
c_4 &= \frac{4(\hat{P^0} - \hat{P^2})(v_+^2 - v_-^2)}{h} + \frac{2(2+\hat{\mu}^2)(2\hat{P^0} - \hat{\mu}^2)(\hat{\mu}^2 - 2\hat{P^0} + h)(v_+ - v_-)}{(2v_+ - \hat{\mu}^2)(2v_- - \hat{\mu}^2)} \\
&\quad - \frac{2[4\hat{P^0}^2(2\hat{P^2} + \hat{\mu}^2) + (\hat{\mu}^2 - r^2)h(2\hat{P^2} + h - 4\hat{P^0}) + h\hat{P^2}(\hat{P^2} + r^2 - 8\hat{P^0})](v_+ - v_-)}{h^2} \\
&\quad - \frac{2}{h}[2(\hat{\mu}^2 - \hat{P^0})(h\hat{\mu}^2 - 2\hat{P^0}h + 4\hat{P^0}^2) + h^2(1 - \hat{P^0} + \hat{\mu}^2) - 2\hat{\mu}^2(r^2 + r^2\hat{P^0} + \hat{P^0}) \\
&\quad + \hat{\mu}^4(1 + r^2 - 2\hat{P^0})] \ln(\frac{2v_+ - \hat{\mu}^2}{2v_- - \hat{\mu}^2}), \qquad (3.20) \\
c_5 &= \frac{2(\hat{\mu}^4 - 4)(\hat{P^2} + r^2 - \hat{\mu}^2)(v_+ - v_-)}{(2v_+ - \hat{\mu}^2)(2v_- - \hat{\mu}^2)} \\
&\quad - \frac{2[\hat{\mu}^2h^2 + (\hat{P^2} + r^2)(2\hat{\mu}^2 + 2h - h^2) + 8r^2\hat{P^2}](v_+ - v_-)}{h^2} \\
&\quad - \frac{2[\hat{\mu}^4h - (\hat{P^2} + r^2)(\hat{\mu}^2h + 4\hat{P^0}) + 2\hat{P^2}\hat{\mu}^2]}{h} \ln(\frac{2v_+ - \hat{\mu}^2}{2v_- - \hat{\mu}^2}). \qquad (3.21)
\end{aligned}
$$

In the expressions for the c_i, we have put $h = \hat{P}^2 - r^2$ and

$$v_\pm = \frac{(\hat{P}^2 + \hat{\mu}^2 - r^2)\hat{P}^0 \pm \sqrt{\hat{P^0}^2 - \hat{P}^2}\sqrt{(\hat{P}^2 + \hat{\mu}^2 - r^2)^2 - 4\hat{\mu}^2\hat{P}^2}}{2\hat{P}^2}. \tag{3.22}$$

The integrals in Eq. (3.12) are done numerically between the kinematic limits

$$\frac{(1-y)^2 + \hat{P}^2}{2(1-y)} \leq \hat{P}^0 \leq \frac{1+\hat{P}^2}{2}, \tag{3.23}$$

$$(\hat{\mu} + r)^2 \leq \hat{P}^2 \leq 1 - y. \tag{3.24}$$

To improve the numerical stability for small $\hat{\mu}^2$, we found it useful to do the $\hat{P}^0$ integral with the variable $\ln(\hat{P}^0 - r^2)$. The remaining limits for this four-body decay are

$$0 \leq \hat{\mu} \leq \sqrt{1-y} - r, \qquad 0 \leq y \leq 1 - r^2. \tag{3.25}$$

3.4 The $\alpha_s^2\beta_0$ correction

Combining the corrections from virtual and real gluon radiation, Eqs. (3.1,3.12), we obtain

$$\frac{d\Gamma^{(1)}(\hat{\mu})}{dy} = \frac{d\Gamma^{(1)}_{virt}(\hat{\mu})}{dy} + \frac{d\Gamma^{(1)}_{brems}(\hat{\mu})}{dy}\Theta(\sqrt{1-y} - r - \hat{\mu}). \tag{3.26}$$

In the $\hat{\mu} \to 0$ limit Eq. (3.26) yields the one-loop correction to the electron spectrum. We have checked that our expression reproduces the result in [17] in this limit. The $\alpha_s^2\beta_0$ part of the two-loop correction is related to the one-loop expression calculated with a massive gluon by [18]

$$\frac{d\Gamma^{(2)}}{dy} = -\frac{\alpha_s^{(V)}\beta_0}{4\pi}\int_0^\infty \frac{d\hat{\mu}^2}{\hat{\mu}^2}\left(\frac{d\Gamma^{(1)}(\hat{\mu})}{dy} - \frac{1}{1+\hat{\mu}^2}\frac{d\Gamma^{(1)}(0)}{dy}\right). \tag{3.27}$$

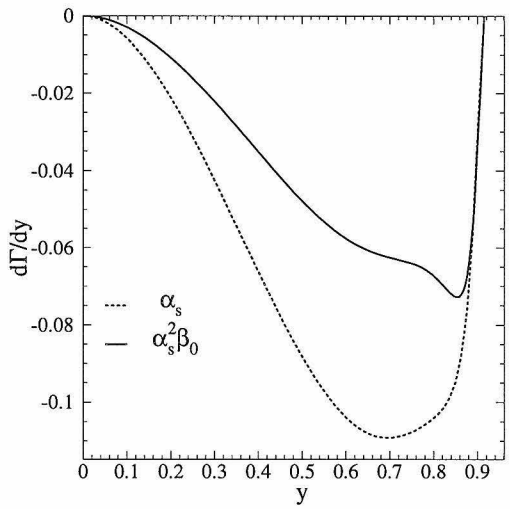

Figure 3.1: Perturbative QCD corrections to the lepton spectrum. The differential rates are given in units of Γ_0, with $r = 0.29$, $\bar{\alpha}_s = 0.2$, and $n_f = 3$.

Note that $\alpha_s^{(V)}$, defined in the V-scheme of BLM [21], is related to the more familiar $\bar{\alpha}_s$ defined in the $\overline{\rm MS}$ scheme by

$$\alpha_s^{(V)} = \bar{\alpha}_s + \frac{5}{3}\frac{\bar{\alpha}_s^2}{4\pi}\beta_0 + \cdots . \tag{3.28}$$

α_s is evaluated at m_b unless stated otherwise. In the $\overline{\rm MS}$ scheme the $\bar{\alpha}_s^2\beta_0$ part of the two-loop correction reads

$$\frac{d\Gamma^{(2)}}{dy} = \frac{5}{3}\frac{\bar{\alpha}_s\beta_0}{4\pi}\frac{d\Gamma^{(1)}(0)}{dy} - \frac{\bar{\alpha}_s\beta_0}{4\pi}\int_0^\infty \frac{d\hat{\mu}^2}{\hat{\mu}^2}\left(\frac{d\Gamma^{(1)}(\hat{\mu})}{dy} - \frac{1}{1+\hat{\mu}^2}\frac{d\Gamma^{(1)}(0)}{dy}\right). \tag{3.29}$$

The dispersion integral has to be done with some care. We found that using $\ln(\hat{\mu}^2)$ instead of $\hat{\mu}^2$ as the integration variable simplifies the numerical evaluation considerably.

In Fig. 3.1 we plot the $\bar{\alpha}_s^2\beta_0$ part of the two-loop correction and for comparison the one-loop correction to the electron spectrum, using $r = 0.29$, $\bar{\alpha}_s = 0.2$, $n_f = 3$,

and dividing by $\Gamma_0 = G_F^2|V_{cb}|^2 m_b^5/192\pi^3$. Except for electron energies close to the endpoint, the $\alpha_s^2\beta_0$ corrections are about half as big as the first order corrections. The perturbation series appears to be controlled, but the higher order corrections clearly are not negligible. Integrating over the electron energy, we reproduce the result for the correction to the total rate given in Ref. [19]. It is worth noting that the $\alpha_s^2\beta_0$ corrections affect the normalization of the differential rate but do not change the shape of the distribution very much. In Section 3.6 we give a polynomial fit to our results that reproduces the numerical results to better than 1% for mass ratios in the range $0.29 \le r \le 0.37$.

3.5 Scalar two- and three-point functions

Here we list expressions for the scalar functions B_0 and C_0 [22] needed for the calculation in this chapter. With the cut for logarithms along the negative real axis, we have

$$\begin{aligned} B_0(a,b,c) &= \frac{2}{\epsilon} - \ln\left(\frac{\mu^2}{4\pi\Lambda^2 e^{-\gamma}}\right) - \int_0^1 dx \ln\left(\frac{ax^2 - x(a+b-c)+b}{\mu^2}\right) \qquad (3.30) \\ &= \frac{2}{\epsilon} - \ln\left(\frac{\mu^2}{4\pi\Lambda^2 e^{-\gamma}}\right) + 2 - \ln\left(\frac{c}{\mu^2}\right) + x_+ \ln\left(\frac{x_+ - 1}{x_+}\right) \\ &\quad + x_- \ln\left(\frac{x_- - 1}{x_-}\right), \qquad (3.31) \end{aligned}$$

where

$$x_\pm = \frac{a+b-c \pm \sqrt{(a+b-c)^2 - 4ab}}{2a}. \qquad (3.32)$$

$$\begin{aligned} C_0(1,\hat{q}^2,r^2 \;,\; \hat{\mu}^2,1,r^2) &= \frac{1}{1+r^2-\hat{q}^2-2\alpha r^2} \times \\ &\Big\{ Li_2\left(\frac{z_1}{z_1-z_4}\right) - Li_2\left(\frac{z_1-1}{z_1-z_4}\right) + Li_2\left(\frac{z_1}{z_1-z_5}\right) \\ &- Li_2\left(\frac{z_1-1}{z_1-z_5}\right) - Li_2\left(\frac{z_2}{z_2-z_6}\right) + Li_2\left(\frac{z_2-1}{z_2-z_6}\right) \\ &- Li_2\left(\frac{z_2}{z_2-z_7}\right) + Li_2\left(\frac{z_2-1}{z_2-z_7}\right) + Li_2\left(\frac{z_3}{z_3-z_8}\right) \end{aligned} \qquad (3.33)$$

$$-Li_2\left(\frac{z_3-1}{z_3-z_8}\right)+Li_2\left(\frac{z_3}{z_3-z_9}\right)-Li_2\left(\frac{z_3-1}{z_3-z_9}\right)\Big\},$$

where

$$\alpha = \frac{(\hat{q}^2-1-r^2)\pm\sqrt{(\hat{q}^2-1-r^2)^2-4r^2}}{-2r^2}, \tag{3.34}$$

$$z_0 = \frac{\hat{\mu}^2-2-\alpha(\hat{q}^2-1-r^2+\hat{\mu}^2)}{1+r^2-\hat{q}^2-2r^2\alpha}, \tag{3.35}$$

$$z_1 = z_0+\alpha, \tag{3.36}$$

$$z_2 = \frac{z_0}{(1-\alpha)}, \tag{3.37}$$

$$z_3 = -\frac{z_0}{\alpha}, \tag{3.38}$$

$$z_{4,5} = \frac{\hat{\mu}^2\pm\sqrt{\hat{\mu}^4-4\hat{\mu}^2r^2}}{2r^2}, \tag{3.39}$$

$$z_{6,7} = \frac{\hat{q}^2+1-r^2\pm\sqrt{(\hat{q}^2+1-r^2)^2-4\hat{q}^2+i\epsilon}}{2\hat{q}^2}, \tag{3.40}$$

$$z_{8,9} = \frac{2-\hat{\mu}^2\pm\sqrt{(2-\hat{\mu}^2)^2-4}}{2}. \tag{3.41}$$

The dilogarithms here are defined as

$$Li_2(z) = -\int_0^1 dt\frac{\ln(1-zt)}{t}. \tag{3.42}$$

3.6 Interpolating function

In this section we give an interpolation scheme that makes it easy to reproduce the $\bar{\alpha}_s^2\beta_0$ corrections to the lepton spectrum for $b\to c\ell\bar{\nu}_\ell$ decays. The interpolation is done as a function of y and r with all other parameters left explicit.

$$\frac{d\Gamma}{dy} = \Gamma_0\left(f^{(0)}(y,r)+\frac{\bar{\alpha}_s}{\pi}f^{(1)}(y,r)+\frac{\bar{\alpha_s^2}\beta_0}{\pi^2}f^{(2)}(y,r)\right). \tag{3.43}$$

The well known tree level result is given by the exact equation

$$f^{(0)}(y,r) = \frac{2y^2(y+r^2-1)^2(-3-3r^2+5y+r^2y-2y^2)}{(y-1)^3}, \tag{3.44}$$

Table 3.1: Coefficients $A_{n,m}$ for the interpolation function $f^{(2)}(y,r)$ given in Section 3.6.

$A_{n,m}$	$m=0$	1	2
$n=1$	−4.9	19.3	−20.4
2	−2.72	12.4	−14.7
3	3.55	−12.4	11.5
4	2.21	−10.1	11.9
5	1.97	−9.59	11.9
6	1.11	−5.08	6.06
7	−0.159	0.448	−0.274
8	−0.336	1.44	−1.62
9	−0.319	1.47	−1.76
10	−0.174	0.818	−0.994
11	−0.0881	0.417	−0.509
12	−0.0507	0.247	−0.309

while the first order function, $f^{(1)}$, can be obtained from Ref. [17]. The interpolating function $f^{(2)}$ is found by fitting Chebyshev polynomials, T_n, to the energy dependence, and quadratic polynomials to the mass ratio r. To improve the accuracy of the fit near the endpoint of the lepton spectrum, the expansion is given in terms of the variable

$$y' = \frac{\ln((1-y)^2/r^2)}{\ln(r^2)}. \tag{3.45}$$

Our fit is accurate to better than 1% for the region

$$0.09 \le y \le 0.99(1-r^2) \qquad 0.29 \le r \le 0.37. \tag{3.46}$$

The second order function is given by

$$f^{(2)}(y,r) = \sum_{n=1}^{12} \left(\sum_{m=0}^{2} A_{n,m}\, r^m \right) T_{n-1}(y'), \tag{3.47}$$

where $T_n(y') = \cos(n \arccos y')$.

The 36 coefficients $A_{i,j}$ are given in Table 3.1. Unfortunately, this interpolation is not accurate enough to calculate the corrections to the moments of the lepton

spectrum we will consider in Chapter 4.

Chapter 4 Applications

4.1 Introduction

In this chapter, we will use the results of the previous two chapters to determine the HQET matrix element λ_1 and the energy of the light degrees of freedom $\bar{\Lambda}$ by comparing observables constructed from the theoretical prediction for the charged lepton spectrum in $B \to X_c \ell \nu$ decays to experimental data. There are several aspects to this. In the first section we will introduce the method and determine the HQET parameters disregarding both the $1/m_b^3$ and the $\alpha_s^2 \beta_0$ corrections but including statistical errors on the experimental side. We also present several checks on the stability of our extraction. The next two sections contain a discussion of the impact of the higher order perturbative and nonperturbative corrections. In the final section we list expressions for the moments of the electron spectrum with various cuts on the lepton energy, which are needed for a more careful analysis currently being done by the CLEO collaboration.

4.2 Moments of the electron spectrum at order $1/m_b^2$ and α_s

The operator product expansion (OPE) shows that in the limit $m_b \gg \Lambda_{\rm QCD}$ inclusive semileptonic B decay rates are equal to the perturbative b quark decay rates [11]. Experimental study of such decays provide measurements of fundamental parameters of the standard model, such as the CKM angles $|V_{cb}|$, $|V_{ub}|$, and the bottom and charm quark masses.

To obtain precise theoretical predictions for inclusive semileptonic B decays, it is important to be able to compute nonperturbative effects suppressed by powers of

$\Lambda_{\rm QCD}/m_b$. [3, 4, 13] The decay rates depend on the quark masses, which can be expressed in terms of the heavy meson masses and the parameters λ_1, λ_2 and $\bar{\Lambda}$. The quantity $\bar{\Lambda}$ [23] also sets the scale for the deviation of the exclusive $B \to D^{(*)}\,\ell\,\bar{\nu}_\ell$ decay form factors from the Isgur-Wise function [1]. The analogue of $\bar{\Lambda}$ in the baryon sector, $\bar{\Lambda}_\Lambda = m_{\Lambda_b} - m_b + \ldots$, describes all $\Lambda_{\rm QCD}/m_Q$ corrections to $\Lambda_b \to \Lambda_c\,\ell\,\bar{\nu}_\ell$ decays [24], and is related to $\bar{\Lambda}$ via $\bar{\Lambda}_\Lambda = \bar{\Lambda} + m_{\Lambda_b} - m_B + \ldots$.

To carry out accurate calculations it is crucial to have reliable determinations of $\bar{\Lambda}$ and λ_1. In the past, these quantities have been estimated using models of QCD [25, 26], and extracting them from experimental data was attempted [27, 28, 29, 30]. Sum rules were also derived to constrain λ_1 [12]. However, perturbative corrections weaken these constraints [31]. In this section we extract $\bar{\Lambda}$ and λ_1 from the shape of the inclusive $B \to X\,\ell\,\bar{\nu}_\ell$ lepton spectrum, and also translate our results into a determination of $|V_{cb}|$, and the $\overline{\rm MS}$ masses $\overline{m}_b(m_b)$, and $\overline{m}_c(m_c)$.

The CLEO Collaboration has measured the inclusive $B \to X\,\ell\,\bar{\nu}_\ell$ lepton spectrum both by demanding only one charged lepton tag [32], and using a double tagged data sample [33] where the charge of a high momentum lepton determines whether the other lepton in the event comes directly from semileptonic B decay (primary) or from the semileptonic decay of a B decay product charmed hadron (secondary). The single tagged data sample has significantly smaller statistical errors, but it is contaminated by secondary leptons below about 1.5 GeV, which cannot be subtracted from the spectrum model independently. The double tagged data sample extends to as low as 0.6 GeV for electrons. For our analysis, we use the single tagged data, which is tabulated in 50 MeV bins in Ref. [34].

The OPE for the lepton spectrum in semileptonic B decay does not reproduce the physical lepton spectrum point-by-point near maximal lepton energy. Near the endpoint comparison with experimental data can only be made after sufficient smearing, or after integrating over a large enough region. The minimal size of this region was estimated to be around $300 - 500$ MeV [3, 4]. This, and the fact that the experimental measurement of the lepton spectrum is precise and model independent only above about 1.5 GeV, impose a limitation on what quantities can be reliably predicted and

compared with data. On the one hand, we want to find observables sensitive to $\bar{\Lambda}$ and λ_1; on the other hand, we want the deviations from the b quark decay prediction to be small, so that the contributions from even higher dimension operators in the OPE are not too important. The observables we use should not depend on $|V_{cb}|$. Thus we consider

$$R_1 = \frac{\int_{1.5\,\mathrm{GeV}} E_\ell \frac{\mathrm{d}\Gamma}{\mathrm{d}E_\ell}\,\mathrm{d}E_\ell}{\int_{1.5\,\mathrm{GeV}} \frac{\mathrm{d}\Gamma}{\mathrm{d}E_\ell}\,\mathrm{d}E_\ell}, \qquad R_2 = \frac{\int_{1.7\,\mathrm{GeV}} \frac{\mathrm{d}\Gamma}{\mathrm{d}E_\ell}\,\mathrm{d}E_\ell}{\int_{1.5\,\mathrm{GeV}} \frac{\mathrm{d}\Gamma}{\mathrm{d}E_\ell}\,\mathrm{d}E_\ell}. \tag{4.1}$$

Before comparing the experimental data with the theoretical predictions for $R_{1,2}$, derived from the OPE and QCD perturbation theory, the following corrections have to be included:

(i) electromagnetic radiative correction

(ii) effects of the boost into the lab frame

(iii) smearing due to the detector momentum resolution.

To take (i) into account, following the CLEO analysis, we used the resummed photon radiation corrections as given in Ref. [35]. These corrections to $R_{1,2}$ have very little sensitivity to subleading logarithms. To determine the corrections due to (ii), we assume that the B mesons are monoenergetic, with energy $m_{\Upsilon(4S)}/2$ (the effect of the 4 MeV spread in the center of mass energy is negligible). We found that the smearing due to the CLEO-II detector momentum resolution [36], and the 50 MeV binning of the data, has a negligible effect on $R_{1,2}$.

Including the nonperturbative corrections up to order $(\Lambda_{\rm QCD}/m_b)^3$ [3, 4, 9] and the order α_s corrections [17], the theoretical expressions for $R_{1,2}$ are

$$\begin{aligned} R_1 \;=\; & 1.8059 - 0.309\,\frac{\bar{\Lambda}}{\overline{m}_B} - 0.35\,\frac{\bar{\Lambda}^2}{\overline{m}_B^2} - 2.32\,\frac{\lambda_1}{\overline{m}_B^2} - 3.96\,\frac{\lambda_2}{\overline{m}_B^2} - 0.4\,\frac{\bar{\Lambda}^3}{\overline{m}_B^3} \\ & - 5.7\,\frac{\bar{\Lambda}\lambda_1}{\overline{m}_B^3} - 6.8\,\frac{\bar{\Lambda}\lambda_2}{\overline{m}_B^3} - 7.7\,\frac{\rho_1}{\overline{m}_B^3} - 1.3\,\frac{\rho_2}{\overline{m}_B^3} - 3.2\,\frac{\mathcal{T}_1}{\overline{m}_B^3} - 4.5\,\frac{\mathcal{T}_2}{\overline{m}_B^3} \\ & - 3.1\,\frac{\mathcal{T}_3}{\overline{m}_B^3} - 4.0\,\frac{\mathcal{T}_4}{\overline{m}_B^3} \end{aligned}$$

$$-\frac{\alpha_s}{\pi}\left(0.035+0.07\,\frac{\bar\Lambda}{\overline{m}_B}\right)+\left|\frac{V_{ub}}{V_{cb}}\right|^2\left(1.33-10.3\,\frac{\bar\Lambda}{\overline{m}_B}\right) \tag{4.2}$$
$$-\left(0.0041-0.004\,\frac{\bar\Lambda}{\overline{m}_B}\right)+\left(0.0062+0.002\,\frac{\bar\Lambda}{\overline{m}_B}\right),$$

$$\begin{aligned} R_2 \;=\;& 0.6581-0.315\,\frac{\bar\Lambda}{\overline{m}_B}-0.68\,\frac{\bar\Lambda^2}{\overline{m}_B^2}-1.65\,\frac{\lambda_1}{\overline{m}_B^2}-4.94\,\frac{\lambda_2}{\overline{m}_B^2}-1.5\,\frac{\bar\Lambda^3}{\overline{m}_B^3} \\ & -7.1\,\frac{\bar\Lambda\lambda_1}{\overline{m}_B^3}-17.5\,\frac{\bar\Lambda\lambda_2}{\overline{m}_B^3}-1.8\,\frac{\rho_1}{\overline{m}_B^3}+2.3\,\frac{\rho_2}{\overline{m}_B^3}-2.9\frac{\mathcal{T}_1}{\overline{m}_B^3}-1.5\frac{\mathcal{T}_2}{\overline{m}_B^3} \\ & -4.0\frac{\mathcal{T}_3}{\overline{m}_B^3}-4.9\frac{\mathcal{T}_4}{\overline{m}_B^3} \\ & -\frac{\alpha_s}{\pi}\left(0.039+0.18\,\frac{\bar\Lambda}{\overline{m}_B}\right)+\left|\frac{V_{ub}}{V_{cb}}\right|^2\left(0.87-3.8\,\frac{\bar\Lambda}{\overline{m}_B}\right) \qquad (4.3) \\ & -\left(0.0073+0.005\,\frac{\bar\Lambda}{\overline{m}_B}\right)+\left(0.0021+0.003\,\frac{\bar\Lambda}{\overline{m}_B}\right), \end{aligned}$$

with R_1 in GeV. We have defined the spin-averaged B meson mass, $\overline{m}_B = (m_B + 3m_{B^*})/4$. The terms in the last two parentheses in each of Eqs. (4.3) and (4.4) represent the effect of the electromagnetic radiative correction, and the effect of the boost into the lab frame, respectively. The parts of these corrections proportional to $\lambda_{1,2}$ are negligible. Eqs. (4.3,4.4) correspond to electrons; for muons the electromagnetic correction is smaller. Corrections to Eqs. (4.3,4.4) of higher order in α_s and $\Lambda_{\rm QCD}/m_b$ will be discussed later. Even though there are no nonperturbative corrections to $R_{1,2}$ of order $\Lambda_{\rm QCD}/m_b$, Eqs. (4.3,4.4) contain terms proportional to $\bar\Lambda/\overline{m}_B$. These arise since we reexpressed the heavy quark masses in terms of hadron masses, using $m_Q = \overline{m}_M - \bar\Lambda + \lambda_1/(2\overline{m}_M)$.

To compare the above theoretical expressions with data, we need to discuss the experimental uncertainties. The central values are $R_1 = 1.7830\,\text{GeV}$ and $R_2 = 0.6108$, while the correlation matrix of the statistical errors [34] is

$$V(R_1,R_2) = \begin{pmatrix} 1.64\times10^{-6} & 2.08\times10^{-6} \\ 2.08\times10^{-6} & 5.45\times10^{-6} \end{pmatrix}. \tag{4.4}$$

Estimating the systematic errors is more complicated. These uncertainties in the lepton spectrum can be divided into two classes: there are additive corrections, like

backgrounds that are subtracted from the data; and there are multiplicative corrections, like those in efficiencies. The total systematic uncertainty in the CLEO measurement of the semileptonic B decay branching fraction is about 2%. However, only a small fraction of these uncertainties affect the shape of the lepton spectrum above 1.5 GeV [37]. In this region the uncertainties in the backgrounds are small, and the efficiencies have fairly flat momentum dependences. While the uncertainties in the electron identification and in the tracking efficiencies are the dominant sources of systematic error in the semileptonic B branching fraction, they are expected to affect $R_{1,2}$ at a much smaller level. We estimate that the systematic uncertainties in $R_{1,2}$ are of comparable size to the statistical errors [37], although a complete analysis of the systematic errors can only be carried out by the CLEO Collaboration. For this reason, and since the statistical errors can be included into our analysis exactly, the experimental uncertainties we shall quote will be the statistical ones only.

In the following discussion we will neglect the $1/m_b^3$ corrections and the $\alpha_s^2\beta_0$ corrections that can be calculated from the results of the previous chapters. These corrections are the subject of the remaining sections in this chapter. The comparison of the theoretical predictions in Eqs. (4.3,4.4) with the CLEO data is shown in Fig. 4.1. The steeper band is the constraint from R_2, while the hatched one is that from R_1. The widths of the bands represent the 1σ statistical errors, while the ellipse shows the 1σ allowed region in $\{\bar{\Lambda}, \lambda_1\}$, after correlations between R_1 and R_2 are taken into account. This region corresponds to $\bar{\Lambda} = 0.39 \pm 0.11\,\text{GeV}$ and $\lambda_1 = -0.19 \pm 0.10\,\text{GeV}^2$. The 1σ allowed region in Fig. 4.1 lies partly within the region allowed by a recent analysis based on moments of the hadron spectrum [30].

In Fig. 4.1 we set $|V_{ub}/V_{cb}| = 0.08$. The extraction of this value is model dependent, and therefore has considerable uncertainty. If $|V_{ub}/V_{cb}| = 0.1$ then the center of the ellipse in Fig. 4.1 would move to $\bar{\Lambda} = 0.42\,\text{GeV}$ and $\lambda_1 = -0.19\,\text{GeV}^2$. We used $\alpha_s = 0.22$, corresponding to the subtraction scale m_b. The sensitivity of our results to this choice of scale is weak; changing α_s to 0.35 moves the central values to $\bar{\Lambda} = 0.36\,\text{GeV}$ and $\lambda_1 = -0.18\,\text{GeV}^2$.

To plot Fig. 4.1 we used the experimental data corresponding to electrons only,

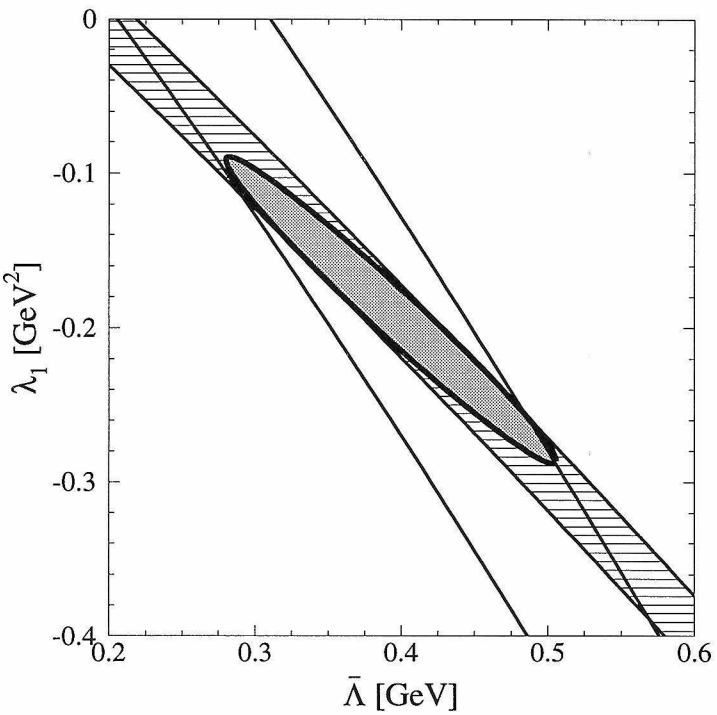

Figure 4.1: Allowed regions in the $\bar{\Lambda} - \lambda_1$ plane for R_1 and R_2. The bands represent the 1σ statistical errors, while the ellipse is the allowed region taking correlations into account. The order $(\Lambda_{\rm QCD}/m_b)^3$ corrections have been omitted.

as we suspect that the systematic uncertainties in the muon data may be larger (for example, the muon detection efficiency is strongly energy dependent below 2 GeV). The latter data set, nevertheless, yields a consistent determination of $\bar{\Lambda}$ and λ_1, giving central values $\bar{\Lambda} = 0.43\,\text{GeV}$ and $\lambda_1 = -0.21\,\text{GeV}^2$ (to subtract secondaries we used the double tagged electron data).

Theoretical uncertainties in this determination of $\bar{\Lambda}$ and λ_1 originate from the reliability of quark-hadron duality at the scales corresponding to the limits in the integrals defining $R_{1,2}$, from order $(\Lambda_{\rm QCD}/m_b)^3$ corrections (see Section 4.5), and from higher order perturbative corrections (see Section 4.3). Concerning duality, note that $E_\ell \geq 1.5\,\text{GeV}$ and $1.7\,\text{GeV}$ (in the lab frame) correspond to summing over hadronic states X with masses below 3.6 GeV and 3.3 GeV, respectively. These scales are likely to be large enough to trust the OPE locally. This is supported

by the fact that a modified ratio that differs from R_2 only in that the integration limit in the numerator is changed from 1.7 GeV to 1.8 GeV yields a parallel band that largely overlaps with that corresponding to R_2. Using this variable and R_1, the central values for $\bar{\Lambda}$ and λ_1 become $\bar{\Lambda} = 0.47\,\text{GeV}$ and $\lambda_1 = -0.26\,\text{GeV}^2$. (The assumption of local duality becomes less reliable using 1.8 GeV.) For higher moments [38] theoretical uncertainties increase, and they are sensitive to an almost identical combination of $\bar{\Lambda}$ and λ_1 as the first moment, R_1. For example, the normalized second moment (with $E_\ell > 1.5\,\text{GeV}$) gives a band that overlaps with that from R_1, and together with R_2 yields the central values $\bar{\Lambda} = 0.39\,\text{GeV}$ and $\lambda_1 = -0.19\,\text{GeV}^2$. Perturbative corrections of order $\alpha_s(\Lambda_{\rm QCD}/m_b)^2$ have not been computed. There is no straightforward way of estimating how they would change the extracted values of $\lambda_1, \bar{\Lambda}$.

$\bar{\Lambda}$ is not a physical quantity, and has a "renormalon ambiguity" of order $\Lambda_{\rm QCD}$ [39]. The perturbative expression for the semileptonic decay rate in terms of the b quark pole mass m_b is not Borel summable, and neither is the perturbative expansion of the $\overline{\rm MS}$ mass $\overline{m}_b(m_b)$ in terms of m_b. These ambiguities cancel if $\bar{\Lambda}$ (or equivalently the b quark pole mass) extracted from the differential semileptonic decay rate is used to get the $\overline{\rm MS}$ mass. Consequently one can arrive at a meaningful prediction for $\overline{m}_b(m_b)$. It is fine to introduce unphysical quantities like $\bar{\Lambda}$, as long as one works consistently to a given order of QCD perturbation theory and the expansion in inverse powers of the heavy quark masses. Since the final results one considers always involve relations between physically measurable quantities, any "renormalon ambiguities" arising from the bad behavior of the QCD perturbation series at large orders cancels out [40].

In summary, using CLEO data on the lepton spectrum from inclusive semileptonic $B \to X\,\ell\,\bar{\nu}_\ell$ decay, we obtained the values of the heavy quark effective theory matrix elements, $\bar{\Lambda} = 0.39 \pm 0.11\,\text{GeV}$ and $\lambda_1 = -0.19 \pm 0.10\,\text{GeV}^2$, where the uncertainty corresponds to the 1σ statistical error. These imply at order α_s that

$$|V_{cb}| = 0.041 \left(\frac{\text{Br}(B \to X_c\,\ell\,\bar{\nu}_\ell)}{0.105} \, \frac{1.54\,\text{ps}}{\tau_B} \right)^{1/2} . \tag{4.5}$$

The difference between the bottom and charm quark pole masses is free of renormalon ambiguities (at order $\Lambda_{\rm QCD}$). We find $m_b - m_c = 3.37 \pm 0.02\,\mathrm{GeV}$, where the uncertainty is the 1σ statistical error. The $\overline{\rm MS}$ quark masses are related to the pole mass via $\overline{m}_Q(m_Q) = m_Q[1 - 4\alpha_s(m_Q)/(3\pi) + \ldots]$. Using this and our values for $\bar{\Lambda}$ and λ_1, we obtain at order α_s

$$\overline{m}_b(m_b) = 4.45\,\mathrm{GeV}\,, \qquad \overline{m}_c(m_c) = 1.28\,\mathrm{GeV}\,. \tag{4.6}$$

Order α_s^2 terms in the relation between m_Q and $\overline{m}_Q(m_Q)$ reduce these $\overline{\rm MS}$ heavy quark masses by about 230 MeV and 160 MeV, respectively. Of course, it is not consistent to use these corrections as order α_s^2 terms have not been included into our determination of $\bar{\Lambda}$ and λ_1 through $R_{1,2}$. Recent determinations of the $\overline{\rm MS}$ b quark mass using lattice QCD are $\overline{m}_b(m_b) = 4.17 \pm 0.06\,\mathrm{GeV}$ and $\overline{m}_b(m_b) = 4.0 \pm 0.1\,\mathrm{GeV}$ [41]. Given the uncertainties in Eq. (4.6) from order α_s^2 effects, our result for $\overline{m}_b(m_b)$ is consistent with these.

The bands in Fig. 4.1 corresponding to $R_{1,2}$ are almost parallel. Hence, even small corrections to Eqs. (4.3,4.4) can significantly affect our determination of $\bar{\Lambda}$ and λ_1. It would be useful to have constraints that depend on very different combinations of $\bar{\Lambda}$ and λ_1. The moments of the photon spectrum in inclusive $B \to X_s\,\gamma$ decay [29] can provide such information.

4.3 The $\alpha_s^2\beta_0$ corrections to the moments

It is straightforward to calculate the $\alpha_s^2\beta_0$ corrections to $R_{1,2}$, using the expressions for the $\alpha_s^2\beta_0$ corrections to the lepton energy spectrum from Section 3.4. Including these corrections has several advantages. Since the $\alpha_s^2\beta_0$ corrections to the spectrum and the total rate are rather substantial, including this contribution may shift the extracted values of $\lambda_1, \bar{\Lambda}$ noticeably. It also allows one to extract the $\overline{\rm MS}$ quark masses at order $\alpha_s^2\beta_0$ in a consistent way. Finally, one can see how well the perturbative series for $R_{1,2}$ converges. In the spirit of HQET, we use the spin averaged meson masses

$\overline{m}_B = 5.314\text{GeV}$, and $\overline{m}_D = 1.975\text{GeV}$ instead of quark masses to compute the $\alpha_s^2\beta_0$ corrections to the moments of the quark level electron spectrum.

Keeping only two-loop corrections that are proportional to β_0, and neglecting terms of order $\alpha_s^2\beta_0\Lambda_{QCD}/\overline{m}_B$ we find

$$\begin{aligned} R_1 &= 1.8059 - 0.035\frac{\alpha_s}{\pi} - 0.082\frac{\alpha_s^2\beta_0}{\pi^2} + \cdots, \\ R_2 &= 0.6581 - 0.039\frac{\alpha_s}{\pi} - 0.098\frac{\alpha_s^2\beta_0}{\pi^2} + \cdots, \end{aligned} \tag{4.7}$$

where the ellipsis denote the other contributions including nonperturbative corrections discussed in [9, 8]. The BLM scales for these quantities are $\mu_{BLM}(R_1) = 0.01\overline{m}_B$, and $\mu_{BLM}(R_2) = 0.007\overline{m}_B$, reflecting the fact that the second order corrections are larger than the first order. This is a result of the almost complete cancellation of the first order perturbative corrections from the denominators and numerators in $R_{1,2}$. In Eq.(4.7) the BLM scales for the numerators and denominators are separately comparable to the BLM scale for the total rate $\mu_{BLM} \approx 0.1\overline{m}_B$. Therefore the very low BLM scales of $R_{1,2}$ do not necessarily indicate badly behaved perturbative series.

In order to demonstrate the impact of the $\alpha_s^2\beta_0$ corrections on the extraction of $\bar{\Lambda}, \lambda_1$, we repeat the analysis of the previous section, neglecting nonperturbative corrections of order $(\Lambda_{QCD}/m_b)^3$. We find that the central values are moved from $\bar{\Lambda} = 0.39 \pm 0.11\text{GeV}$, $\lambda_1 = -0.19 \pm 0.10\text{GeV}^2$ to $\bar{\Lambda} = 0.33\text{GeV}$, $\lambda_1 = -0.17$. The shift in the values of the HQET matrix elements lies well within the 1σ statistical error of the previously extracted values, indicating that the perturbative series for $\lambda_1, \bar{\Lambda}$ in terms of the experimentally measured values of $R_{1,2}$ converges better than that of the individual moments, Eq. (4.7).

Using the values of the HQET matrix elements extracted at a given order in α_s, to predict physical observables at the same order in α_s, guarantees that the renormalon ambiguity in $\bar{\Lambda}$ and λ_1 will cancel [42, 43] if the expansion is continued to sufficiently high orders in α_s. Thus including the $\alpha_s^2\beta_0$ parts in the determination of $\bar{\Lambda}, \lambda_1$ allows one to calculate the $\overline{\text{MS}}$ quark masses consistently at order $\alpha_s^2\beta_0$. To second order in

Λ_{QCD}/m_q and to order $\alpha_s^2\beta_0$ we have

$$\overline{m}_q(m_q) = \left(\overline{m}_{Meson} - \bar{\Lambda} + \frac{\lambda_1}{2m_q} + \cdots\right)\left(1 - \frac{4\alpha_s(m_q)}{3\pi} - 1.56\frac{\alpha_s^2(m_q)\beta_0}{\pi^2} + \cdots\right), \tag{4.8}$$

where m_q is the b or c quark pole mass and $\overline{m}_{Meson}$ is the corresponding spin averaged meson mass. With $\alpha_s(m_b) = 0.22$, $\alpha_s(m_c) = 0.39$ this yields $\overline{m}_b(m_b) = 4.16\text{GeV}, \overline{m}_c(m_c) = 0.99\text{GeV}$ for the $\overline{\text{MS}}$ quark masses, albeit with large theoretical uncertainties due to the effect of the higher order nonperturbative corrections on the extraction of $\bar{\Lambda}, \lambda_1$[9]. The value of $\overline{m}_b(m_b)$ is in good agreement with lattice calculations $\overline{m}_b(m_b) = 4.17 \pm 0.06\text{GeV}$ and $\overline{m}_b(m_b) = 4.0 \pm 0.01\text{GeV}$[41]. The weak mixing angle $|V_{cb}|$ can be determined by comparing the theoretical prediction for the total rate with experimental measurements. Including all corrections discussed in the previous section we find at order $\alpha_s^2\beta_0$

$$|V_{cb}| = 0.043\left(\frac{Br(B \to X_c\ell\bar{\nu}_\ell)}{0.105}\frac{1.55\text{ps}}{\tau_B}\right)^{1/2}. \tag{4.9}$$

4.4 Quark model estimates for the $\mathcal{T}_i$

The $1/m_b^3$ contributions to the lepton and hadron spectra from inclusive B decay are parametrized by the expectation values of two local (ρ_1, ρ_2) and four nonlocal ($\mathcal{T}_1 - \mathcal{T}_4$) operators. To use our results on the $1/m_b^3$ corrections to the differential decay rates to assess the theoretical uncertainties in the extraction of $\lambda_1, \bar{\Lambda}$, we need to estimate the size of these expectation values. If one wants to do better than just use dimensional analysis, one is forced to leave the safe ground of HQET and the OPE and resort to models of QCD. We chose the ISGW model [44] updated in Ref. [45] as the most suitable for our purposes. ISGW is a nonrelativistic quark model which is designed to describe the ground and the low-lying excited states of heavy-light mesons. The heavy-light meson is thought of as a bound system of a heavy quark of mass m_b and

a constituent light quark of mass m_q interacting via the "Cornell" potential

$$V(r) = -\frac{4\alpha_s}{3r} + c + br. \tag{4.10}$$

We take $m_b = 5.2$ GeV, $m_q = 0.33$ GeV, $\alpha_s = 0.5, c = -0.81$ GeV, $b = 0.18$ GeV^2, as in Ref. [45]. This set of parameters reproduces well the spin-averaged masses of the $1S$ and $1P$ heavy-light mesons. The same potential also describes satisfactorily the spectrum of light-light and heavy-heavy mesons. In the spirit of HQET, we will treat the kinetic energy of the b quark as a perturbation. In order to mimic the spin-symmetry violating effects, we include the spin-spin Hamiltonian [45]

$$H_{ss} = \frac{32\pi a\alpha_s}{9m_q m_b}\left[\frac{m_q}{E_q}\right]^{1/2} \mathbf{S}_b \cdot \mathbf{S}_q \delta^3(\mathbf{r}) \left[\frac{m_q}{E_q}\right]^{1/2}, \tag{4.11}$$

where $\mathbf{S}_q$ and $\mathbf{S}_b$ are spin operators of the constituent quark and heavy quark respectively, and $E_q = \sqrt{\mathbf{p}^2 + m^2}$. The value of a is chosen so as to reproduce the observed hyperfine splittings. In Ref. [45] a was taken to be 2.8. However, we found that the simple variational ansatz for the wavefunction adopted in Refs. [44, 45] substantially underestimates the magnitude of the wavefunction at the origin, resulting in an overestimate of a. Using numerical solutions of the Schrödinger equation, we find that $a = 1.6$ reproduces the observed hyperfine splitting in heavy-light mesons. Thus we will take $a = 1.6$ and use the numerical solutions in the subsequent analysis.

We begin by estimating λ_1 in the ISGW model (there is no need to compute λ_2, since the model was tailored to get the correct $B - B^*$ splitting):

$$\lambda_1 = -\langle\, \mathbf{p}^2 \,\rangle \simeq -0.27\text{GeV}^2. \tag{4.12}$$

We will see in the next section that this result lies within the range of values extracted from the lepton spectrum in inclusive B-decay.

Let us turn now to dimension-six operators. Using the equations of motion for the heavy field h_v and switching to the first-quantized formalism, we can rewrite the

definition of ρ_1 in the following form:

$$\rho_1 = -\frac{1}{2}\langle\,[\,\mathbf{p},[\,\mathbf{p},V(r)]\,]\,\rangle = \frac{1}{2}\langle\,\nabla^2 V(r)\,\rangle. \tag{4.13}$$

Evaluating this expectation value for the ground state of the B meson, we find

$$\rho_1 \simeq 0.20\mathrm{GeV}^3. \tag{4.14}$$

This estimate is larger than those obtained from the vacuum-saturation approximation [46, 12, 14, 47, 8]. However, two important points were not appreciated in Ref. [8], where the rather low value, $\rho_1 \simeq 0.03$ GeV^3, was found. First, in the vacuum-saturation estimate, $\rho_1 = (2\pi\alpha_s/9)m_B f_B^2$, f_B should be understood as the decay constant in the static limit of HQET, rather than in the full theory. This distinction is important, since lattice simulation indicate that $f_B \simeq 270$ MeV in the static limit, while in the full theory we have $f_B \simeq 190$ MeV. Second, the above estimate contains α_s at some undetermined scale μ. In Ref. [8] μ was taken to be the highest scale in the problem, m_b, without serious justification. If instead one takes μ to be lower, as suggested in Refs. [46, 16], one obtains larger values for ρ_1. For example, for $\mu \simeq 1$ GeV we get $\rho_1 \simeq 0.12$ GeV^3.

Sum rules in the small velocity limit can also be used to estimate ρ_1 [47]. This approach also gives values smaller than the quark model. This may be due to saturating the sum over the exclusive channels by the two lowest resonances.

The matrix element ρ_2 can be rewritten as

$$\rho_2 = -\frac{1}{3}\langle\,\mathbf{S}_b\cdot(g\mathbf{E}(0)\times\mathbf{p})\,\rangle. \tag{4.15}$$

Since in our model $g\mathbf{E} = -\nabla V(r)$, we see that for $L = 0$ states ρ_2 is zero. This is, of course, a reflection of the nonrelativistic character of the ISGW model, which treats spin-orbit interactions as negligible. Since the model seems to describe the meson spectrum rather well, we take this as an indication that ρ_2 is small on the scale suggested by the dimensional analysis. However, a possible viewpoint is that

the nonrelativistic quark model is inherently unable to make a prediction for ρ_2.

To evaluate $\mathcal{T}_1 - \mathcal{T}_4$, we insert a complete set of states between the two operators in Eqs. (2.53). Note that the kinetic energy operator, and the hyperfine operator Eq. (4.11) which is the quark-model analog of $\sigma\mathbf{B}/2m_b$, commute with the orbital angular momentum. Thus only radially excited states will contribute to the sum over intermediate states. Therefore, $\mathcal{T}_1 - \mathcal{T}_4$ reduce to

$$\mathcal{T}_1 = \sum_{n>1} \frac{|\langle 1S|\mathbf{p}^2|nS\rangle|^2}{E_n - E_1}, \tag{4.16}$$

$$\mathcal{T}_2 = -\sum_{n>1} \frac{\langle 1S|\mathbf{p}^2|nS\rangle\langle nS|O_{ss}|1S\rangle}{E_n - E_1} + h.c., \tag{4.17}$$

$$\mathcal{T}_3 = 12\sum_{n>1} \frac{|\langle 1S|O_{ss}|nS\rangle|^2}{E_n - E_1}, \tag{4.18}$$

$$\mathcal{T}_4 = \mathcal{T}_2 + \frac{2}{3}\mathcal{T}_3. \tag{4.19}$$

Here O_{ss} is defined as

$$O_{ss} = \frac{8\pi a\alpha_s}{9m_q}\left[\frac{m_q}{E_q}\right]^{1/2}\delta^3(\mathbf{r})\left[\frac{m_q}{E_q}\right]^{1/2}. \tag{4.20}$$

We computed the sums numerically, including the first eight radially excited states, and obtained the following estimates for $\mathcal{T}_1 - \mathcal{T}_4$:

$$\mathcal{T}_1 \simeq 0.08\text{GeV}^3, \quad \mathcal{T}_2 \simeq -0.04\text{GeV}^3, \quad \mathcal{T}_3 \simeq 0.07\text{GeV}^3, \quad \mathcal{T}_4 \simeq 0.01\text{GeV}^3. \tag{4.21}$$

The rate of convergence of the sum over intermediate states may serve to a certain extent as an indicator of reliability of the above results. If the sum is dominated by a few low-lying states, one may hope that the quark model correctly describes them. On the other hand, the highly excited states in the quark model have little resemblance to excited states in real QCD. It turns out that $\mathcal{T}_1$ and $\mathcal{T}_2$ are essentially saturated (to an accuracy of about 20%) by the two lowest excited states, while for $\mathcal{T}_3$ (and hence for $\mathcal{T}_4$) the convergence is much slower. For example, retaining only

the first two excited states gives $\mathcal{T}_3 \simeq 0.04\text{GeV}^3, \mathcal{T}_4 \simeq -0.004\text{GeV}^3$. Thus the quark model estimates for the latter two matrix elements should be taken with a grain of salt.

One should realize that even if the sum over intermediate states converged rapidly, the quark model estimates of $\mathcal{T}_3$ and $\mathcal{T}_4$ would be on a shakier ground than those of the other matrix elements, since the hyperfine Hamiltonian we used does not have a "tensor" part, and thus commutes with the orbital angular momentum. In Ref. [44] one was interested only in the diagonal elements of the hyperfine Hamiltonian in the S-states, and thus the "tensor" part did not matter. However, on general grounds one does not expect the "tensor" interactions to be negligible, in which case the orbital excitations will contribute to $\mathcal{T}_3$ and $\mathcal{T}_4$. In contrast, only radial excitations contribute to $\mathcal{T}_2$, irrespective of the form of the hyperfine Hamiltonian, which indicates that it can be predicted more reliably than $\mathcal{T}_{3,4}$.

4.5 Implications of the $1/m_b^3$ corrections

The $1/m_b^3$ corrections to the electron spectrum shift the predicted values of $R_{1,2}$ by amounts that are parametrized by the two local matrix elements ρ_1, ρ_2 and the nonlocal matrix elements $\mathcal{T}_i$. Since the bands in the $\lambda_1 - \bar{\Lambda}$ plane we get from $R_{1,2}$ are almost parallel, the intersection of these bands can be shifted substantially by small corrections to the moments. In this section we will show how much the unknown $1/m_b^3$ corrections weaken the extraction of $\lambda_1, \bar{\Lambda}$. We will do this using dimensional analysis to estimate the size of the higher order matrix elements and also show the results if the quark model estimates in the previous section are taken seriously. In the analysis below we will not include the $\alpha_s^2\beta_0$ corrections to $R_{1,2}$ since these corrections are vanishingly small relative to the uncertainty from the $1/m_b^3$ corrections. However, if one wants to include them approximately, one can shift the extracted values of $\lambda_1, \bar{\Lambda}$ by the same amount as they were shifted in Section 4.3.

In order to take the uncertainties from the higher order matrix elements into account, we equate the expressions for $R_{1,2}$ to the experimental values using $|V_{ub}/V_{cb}| =$

$0.08, \alpha_s = 0.22$ and Eqs. (2.62) to eliminate λ_2 and ρ_2. This yields the extracted values of $\bar{\Lambda}, \lambda_1$ in the form

$$\begin{aligned} \bar{\Lambda} &= f_{\bar{\Lambda}}(R_1^{exp}, R_2^{exp}, \rho_1, \mathcal{T}_1, \mathcal{T}_2, \mathcal{T}_3, \mathcal{T}_4) \\ \lambda_1 &= f_{\lambda_1}(R_1^{exp}, R_2^{exp}, \rho_1, \mathcal{T}_1, \mathcal{T}_2, \mathcal{T}_3, \mathcal{T}_4). \end{aligned} \tag{4.22}$$

Dimensional analysis suggests that the higher order matrix elements are all of order Λ_{QCD}^3, which can be used to make a quantitative estimate of the uncertainties in the extraction of $\bar{\Lambda}, \lambda_1$. We vary the magnitude of $\rho_1, \mathcal{T}_1 - \mathcal{T}_4$ in Eqs. (4.22) independently in the range $0 - (0.5\text{GeV})^3$, taking ρ_1 to be positive, as indicated by the vacuum saturation approximation, but making no assumption about the sign of the other matrix elements. Using the central values for $R_{1,2}^{exp}$, we find that $\bar{\Lambda}, \lambda_1$ can lie inside the shaded region in Fig. 4.2. For comparison we also display the values of $\bar{\Lambda}, \lambda_1$ extracted in Ref. [8] together with the ellipse showing the size of the statistical error of the experimental data. Clearly the theoretical uncertainties dominate the accuracy to which $\bar{\Lambda}, \lambda_1$ can be extracted.

The situation can be improved only if we have some independent information on some or all of the higher dimension matrix elements. This requires either more experimental input or theoretical estimates of these matrix elements. ρ_1 can be estimated in the vacuum saturation approximation [48, 46, 12, 14, 47, 8], $\rho_1 = (2\pi\alpha_s/9) m_B f_B^2$. The numerical value obtained this way is rather uncertain. Taking $\alpha_s = 0.5$ and $f_B = 270\text{MeV}$ for purposes of illustration, we find $\rho_1 \simeq 0.13\text{GeV}^3$. No similar estimates exist for the other dimension-six matrix elements. ρ_2 vanishes in any non relativistic potential model, which may be taken as an indication that it is small relative to the other matrix elements.

The cross hatched region in Fig. 4.2 shows the range of $\bar{\Lambda}, \lambda_1$ one obtains from setting $\rho_1 = 0.13\text{GeV}^3$ and $\rho_2 = 0$ and varying the magnitude of the other matrix elements in the range $0 - (0.5\text{GeV})^3$. The previously extracted values of $\bar{\Lambda}, \lambda_1$ are not excluded by this choice of $\rho_{1,2}$.

Alternatively, we can use the quark model estimates of the higher dimension ma-

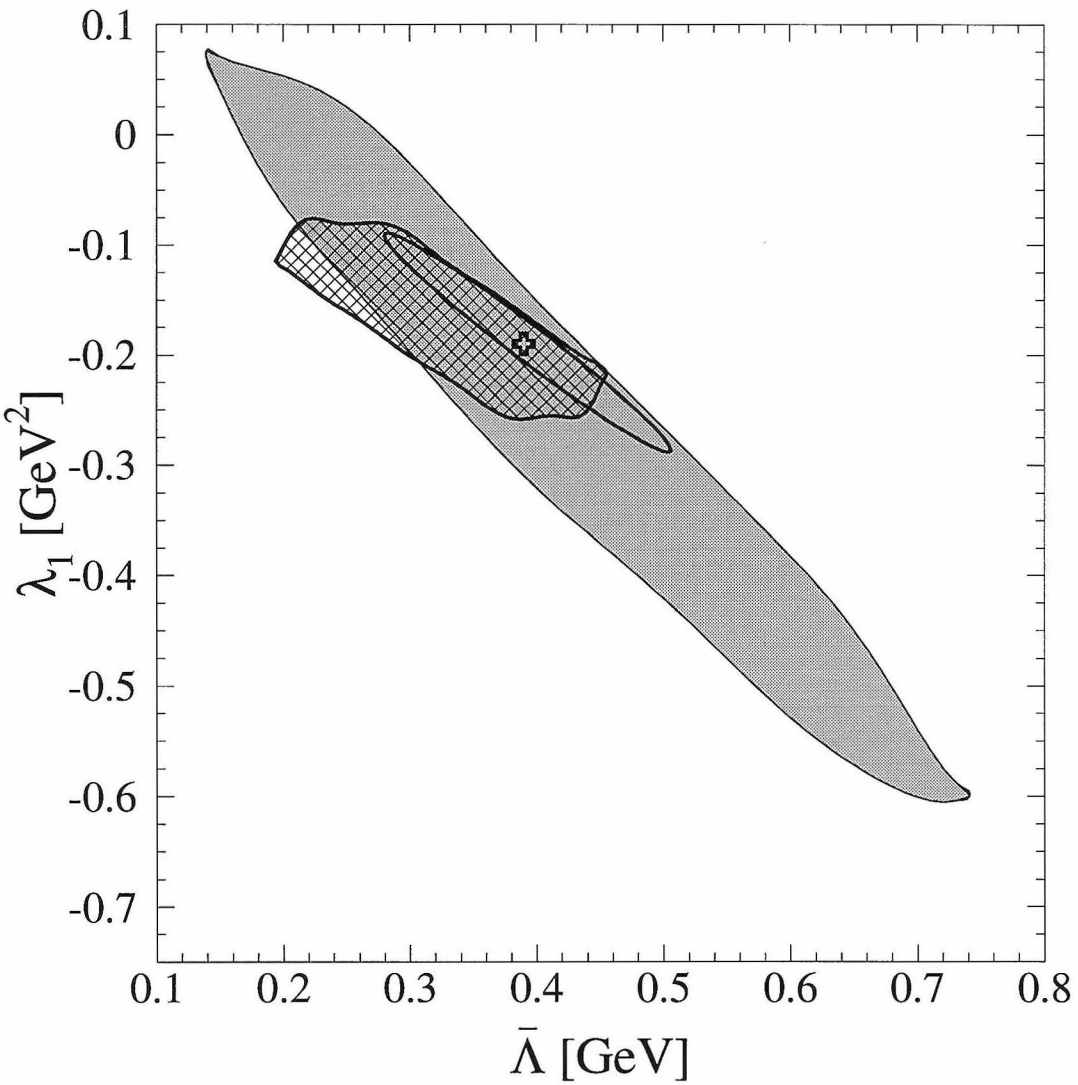

Figure 4.2: Impact of $1/m_b^3$ corrections on the extraction of $\bar{\Lambda}, \lambda_1$. Shaded region: Higher order matrix elements estimated by dimensional analysis. Cross-hatched region: $\rho_1 = 0.13\text{GeV}^3$, $\rho_2 = 0$. Cross and ellipse show the values of $\bar{\Lambda}, \lambda_1$ extracted without $1/m_b^3$ corrections but including the experimental statistical error.

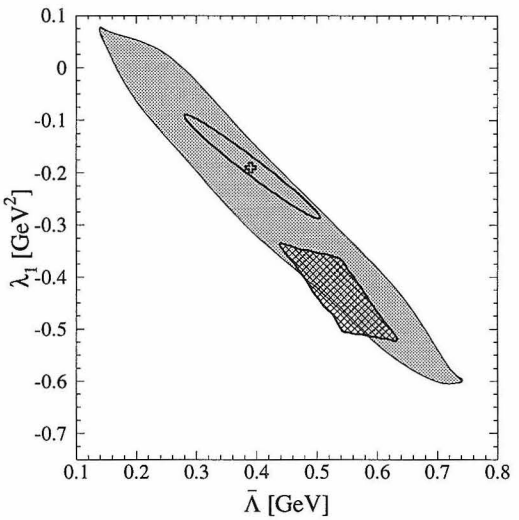

Figure 4.3: Impact of $1/m_b^3$ corrections on the extraction of $\bar{\Lambda}, \lambda_1$. Shaded region: Higher order matrix elements estimated by dimensional analysis. Cross-hatched region: $\rho_1 = 0.13\text{GeV}^3$, $\rho_2 = 0$, $\mathcal{T}_{1,2}$ from quark model. Cross and ellipse show the values of $\bar{\Lambda}, \lambda_1$ extracted without $1/m_b^3$ corrections but including the experimental statistical error.

trix elements from Section 4.4, keeping the caveats mentioned there in mind. Since the predictions for $\mathcal{T}_3$ and $\mathcal{T}_4$ are even less reliable than those for ρ_1 and $\mathcal{T}_{1,2}$, we vary their value in the range $0 - (0.5\text{GeV})^3$ as before and use the quark model values of $\rho_1, \mathcal{T}_{1,2}$. This results in the crosshatched region in Fig. 4.3. The high value ρ_1 in the quark model causes this region to lie partially outside the region suggested by dimensional analysis.

This method of extracting $\bar{\Lambda}, \lambda_1$ is especially sensitive to higher order corrections since the constraints obtained form R_1 and R_2 give almost parallel bands in the $\bar{\Lambda} - \lambda_1$ plane. Thus small uncertainties in the theoretical expressions for $R_{1,2}$ result in large uncertainties in the extracted values of $\bar{\Lambda}, \lambda_1$. The same applies to the very similar analysis in Ref. [49]. The rare decay $B \to X_s\gamma$ provides a way to extract a vertical band in the $\bar{\Lambda} - \lambda_1$ plane, but at present the experimental data does not allow a quantitative analysis [29]. Furthermore, it is not clear when HQET matrix elements extracted from different observables can be compared meaningfully [42, 30].

4.6 Moments of the hadronic invariant mass spectrum

The second method for extracting information on $\bar{\Lambda}, \lambda_1$ [30] was used to exclude some regions in the $\bar{\Lambda} - \lambda_1$ plane. The first and second moments of the invariant mass spectrum of the hadrons in the final state of the inclusive decay $B \to X_c \ell \nu$ turn out to give independent constraints on $\bar{\Lambda}, \lambda_1$. Their definition involves the total decay rate at order $1/\overline{m}_B^3$. It can be obtained by combining the total rate at order $1/m_b^2$ from Ref. [3] with the contributions from local dimension-six operators Eq. (2.63) and using Eqs. (2.54). Finally Eqs. (2.59) and (2.60) are used to eliminate the quark masses. Using the measured values for the meson masses and neglecting perturbative corrections, we find to third order in $1/\overline{m}_B$:

$$\Gamma = \frac{|V_{cb}|^2 G_F^2 \overline{m}_B^5}{192\pi^3}\left[0.3689 - 0.6080\frac{\bar{\Lambda}}{\overline{m}_B} - 0.349\frac{\bar{\Lambda}^2}{\overline{m}_B^2} - 1.175\frac{\lambda_1}{\overline{m}_B^2} - 2.757\frac{\lambda_2}{\overline{m}_B^2}\right. \quad (4.23)$$

$$-0.11\frac{\bar{\Lambda}^3}{\overline{m}_B^3} - 1.21\frac{\bar{\Lambda}\lambda_1}{\overline{m}_B^3} + 2.95\frac{\bar{\Lambda}\lambda_2}{\overline{m}_B^3} - 2.27\frac{\rho_1}{\overline{m}_B^3} + 2.76\frac{\rho_2}{\overline{m}_B^3} - 2.73\frac{\mathcal{T}_1}{\overline{m}_B^3} \quad (4.24)$$

$$\left. +0.55\frac{\mathcal{T}_2}{\overline{m}_B^3} - 3.84\frac{\mathcal{T}_3}{\overline{m}_B^3} - 2.76\frac{\mathcal{T}_4}{\overline{m}_B^3}\right].$$

Since none of the coefficients of the higher order matrix elements turn out to be abnormally large, dimensional analysis indicates that the $1/\overline{m}_B^3$ corrections to the total rate should not exceed 2%.

The hadronic moments are defined as

$$\langle (s_H - \overline{m}_D^2)^n \rangle = \frac{1}{\Gamma}\int \mathrm{d}s_H \mathrm{d}E_H (s_H - \overline{m}_D^2)^n \frac{\mathrm{d}\Gamma}{\mathrm{d}s_H \mathrm{d}E_H}, \quad (4.25)$$

where $s_H = m_B^2 - 2m_B v \cdot q + q^2$ and $E_H = m_B - v \cdot q$ are the hadronic analogs of $\hat{s}_0, \hat{E}_0$ defined in Section 2.3. Using the relation between quark and hadron masses, one can relate s_H, E_H to $\hat{s}_0, \hat{E}_0$ and thus compute the moments using the expressions given in Ref. [30] together with Eq. (2.46) and the usual substitution Eqs. (2.54). We

find to order $1/\overline{m}_B^3$:

$$\begin{aligned}
\langle s_H - \overline{m}_D^2 \rangle &= \overline{m}_B^2 \Big[0.051 \frac{\alpha_s}{\pi} + 0.23 \frac{\bar{\Lambda}}{\overline{m}_B} \left(1 + 0.43 \frac{\alpha_s}{\pi} \right) \\
&\quad + 0.26 \frac{1}{\overline{m}_B^3} (\bar{\Lambda}^2 + 3.9\lambda_1 - 1.2\lambda_2) \\
&\quad + 0.33 \frac{1}{\overline{m}_B^3} (\bar{\Lambda}^3 + 6.6\bar{\Lambda}\lambda_1 - 1.7\bar{\Lambda}\lambda_2 + 7.0\rho_1 + 3.5\rho_2 \\
&\quad + 5.0\mathcal{T}_1 + 2.5\mathcal{T}_2 + 4.6\mathcal{T}_3 + 1.3\mathcal{T}_4) \Big] \qquad (4.26) \\
\langle (s_H - \overline{m}_D^2)^2 \rangle &= \overline{m}_B^4 \Big[0.0053 \frac{\alpha_s}{\pi} + 0.038 \frac{\bar{\Lambda}}{\overline{m}_B} \frac{\alpha_s}{\pi} + 0.065 \frac{1}{\overline{m}_B^3} (\bar{\Lambda}^2 - 2.1\lambda_1) \\
&\quad + 0.14 \frac{1}{\overline{m}_B^3} (\bar{\Lambda}^3 + 2.2\bar{\Lambda}\lambda_1 + 2.2\bar{\Lambda}\lambda_2 - 6.0\rho_1 + 1.7\rho_2 \\
&\quad - 1.0\mathcal{T}_1 - 2.9\mathcal{T}_2) \Big] \qquad (4.27)
\end{aligned}$$

where perturbative α_s corrections have been included. Rather than repeating the analysis presented in Ref. [30], we use these expressions to predict the values of the hadronic moments using the HQET matrix elements extracted from the lepton energy spectrum. The main reason for doing this is that the experimental measurement of the necessary branching fractions is not very precise. In particular ALEPH and CLEO quote only an upper bound for $Br(B \to D_2^* \ell \bar{\nu})$ [50, 51]. We extract an upper bound on this branching fraction from the theoretical prediction of the hadronic moments. A lower bound for the first hadronic moment is given by [30]

$$\begin{aligned}
\langle s_H - \overline{m}_D^2 \rangle &\geq a \Big[(2.450\text{GeV})^2 - (1.975\text{GeV})^2 \Big] + b \Big[(2.010\text{GeV})^2 - (1.975\text{GeV})^2 \Big] \\
&\quad + c \Big[(1.869\text{GeV})^2 - (1.975\text{GeV})^2 \Big] \qquad (4.28)
\end{aligned}$$

where a, b, and c are the semileptonic branching fractions to D^{**}, D^*, and D relative to the total semileptonic branching fraction. Using the measured ratio 0.41:0.59 for the decays to D and D^*, we can write b, c as functions of the branching fraction a for D^{**}:

$$b = 0.59(1-a), \qquad c = 0.41(1-a) \qquad (4.29)$$

We take $a+b+c=1$, which is appropriate because we need only a lower bound on the hadronic moment. It is also implicitly assumed that the nonresonant semileptonic branching fraction below the D^{**} mass is negligible. Similarly, for the second hadronic moment we take

$$\langle (s_H - \overline{m}_D^2)^2 \rangle \geq a \left[(2.450\text{GeV})^2 - (1.975\text{GeV})^2 \right]^2 , \tag{4.30}$$

where small contributions from the ground state mesons D, D^* have been neglected. We obtain theoretical predictions for the hadronic moments by substituting values of $\rho_1, \mathcal{T}_1 - \mathcal{T}_4$ and the corresponding values of $\bar{\Lambda}, \lambda_1$ extracted from the lepton spectrum into Eqs. (4.26). As before, we allow the magnitudes of ρ_1 and $\mathcal{T}_1 - \mathcal{T}_4$ to vary in the range $0 - (0.5\text{GeV})^3$ with ρ_1 being positive. Imposing the constraint that the largest values of the hadronic moments obtained from this procedure be larger than the lower bounds Eqs. (4.28),(4.30), we find the upper bound on the D^{**} branching fraction

$$a \leq 0.23 . \tag{4.31}$$

This value is compatible with the experimentally measured values from ALEPH [50] ($Br(B \to D_1 \ell\nu) = 0.069 \pm 0.015, Br(B \to D_2^* \ell\nu) < 0.11$) and from CLEO[51]($Br(B \to D_1 \ell\nu) = 0.046 \pm 0.013, Br(B \to D_2^* \ell\nu) < 0.11$). It is also marginally consistent with the OPAL result $a = 0.34 \pm 0.07$[52]. Unless the matrix elements of dimension-six operators are even bigger than we have assumed, this implies that the branching fraction $a = 0.27$ used in [30] is inconsistent with the values of $\bar{\Lambda}, \lambda_1$ extracted from the lepton spectrum.

4.7 Moments with other cuts

Recently the CLEO collaboration has begun an analysis very similar to what we have presented in this chapter. They will be able to use the double tagged lepton spectrum for their analysis since they now have sufficient numbers of events to reduce the statistical errors significantly. Specifically, they will measure the first and second

moment of the electron spectrum,

$$M_n = \frac{\int_C E_\ell^n \frac{\mathrm{d}\Gamma}{\mathrm{d}E_\ell}\,\mathrm{d}E_\ell}{\int_C \frac{\mathrm{d}\Gamma}{\mathrm{d}E_\ell}\,\mathrm{d}E_\ell}, \tag{4.32}$$

down to 0.6GeV and expect to have a reliable extrapolation to zero lepton energy. In view of this it is useful to have theoretical predictions for $M_{1,2}$ (M_1 is identical to R_1) without cut on the lepton energy and with a cut at 0.6GeV. Comparing extractions of $\lambda_1, \bar{\Lambda}$ using these two sets of moments will provide a check on the quality of the extrapolation. Comparing the values of $\lambda_1, \bar{\Lambda}$ from these moments with those from moments with a 1.5GeV cut can ascertain whether there are any significant violations of quark hadron duality in the range 0.6-1.5GeV. Since no data are available so far, we only give the theoretical expressions for $M_{1,2}$. Without cut ($C = 0$) we find

$$\begin{aligned}
M_1 \;=\;& 1.4289 - 0.6\frac{\bar{\Lambda}^3}{\overline{m}_B^3} - 5.3\frac{\bar{\Lambda}\lambda_1}{\overline{m}_B^3} - 8.1\frac{\bar{\Lambda}\lambda_2}{\overline{m}_B^3} - 0.40\frac{\bar{\Lambda}^2}{\overline{m}_B^2} - 2.10\frac{\lambda_1}{\overline{m}_B^2} \\
& -5.16\frac{\lambda_2}{\overline{m}_B^2} - 0.289\frac{\bar{\Lambda}}{mB} - 5.1\frac{\rho_1}{\overline{m}_B^3} + 1.7\frac{\rho_2}{\overline{m}_B^3} - 3.5\frac{\mathcal{T}_1}{\overline{m}_B^3} - 2.1\frac{\mathcal{T}_2}{mB^3} \\
& -4.5\frac{\mathcal{T}_3}{\overline{m}_B^3} - 5.2\frac{\mathcal{T}_4}{\overline{m}_B^3} \\
& +\frac{\alpha_s}{\pi}\left(-0.002 - 0.07\frac{\bar{\Lambda}}{\overline{m}_B}\right) + \frac{\alpha_s^2\beta_0}{\pi^2}(-0.070) + \left|\frac{V_{ub}}{V_{cb}}\right|^2\left(1.17 - 8.2\frac{\bar{\Lambda}}{\overline{m}_B}\right) \\
& +\left(-0.0151 + 0.002\frac{\bar{\Lambda}}{\overline{m}_B}\right) + \left(0.0030 - 0.001\frac{\bar{\Lambda}}{\overline{m}_B}\right)
\end{aligned} \tag{4.33}$$

$$\begin{aligned}
M_2 \;=\;& 2.23978 - 1.6\frac{\bar{\Lambda}^3}{\overline{m}_B^3} - 16.0\frac{\bar{\Lambda}\lambda_1}{\overline{m}_B^3} - 22.4\frac{\bar{\Lambda}\lambda_2}{\overline{m}_B^3} - 1.16\frac{\bar{\Lambda}^2}{\overline{m}_B^2} - 7.21\frac{\lambda_1}{\overline{m}_B^2} \\
& -16.34\frac{\lambda_2}{\overline{m}_B^2} - 0.975\frac{\bar{\Lambda}}{\overline{m}_B} - 20.2\frac{\rho_1}{\overline{m}_B^3} + 3.2\frac{\rho_2}{\overline{m}_B^3} - 11.4\frac{\mathcal{T}_1}{\overline{m}_B^3} - 9.0\frac{\mathcal{T}_2}{\overline{m}_B^3} \\
& -13.9\frac{\mathcal{T}_3}{\overline{m}_B^3} - 16.3\frac{\mathcal{T}_4}{\overline{m}_B^3} \\
& +\frac{\alpha_s}{\pi}\left(-0.033 - 0.07\frac{\bar{\Lambda}}{\overline{m}_B}\right) + \frac{\alpha_s^2\beta_0}{\pi^2}(-0.24) + \left|\frac{V_{ub}}{V_{cb}}\right|^2\left(4.14 - 31.6\frac{\bar{\Lambda}}{\overline{m}_B}\right) \\
& +\left(-0.0415 + 0.015\frac{\bar{\Lambda}}{\overline{m}_B}\right) + \left(0.0126 - 0.006\frac{\bar{\Lambda}}{\overline{m}_B}\right)
\end{aligned} \tag{4.34}$$

With a cut at 0.6GeV ($C = 0.6$GeV) the moments are given by

$$\begin{aligned}
M_1 &= 1.4756 - 0.6\frac{\bar{\Lambda}^3}{\overline{m}_B^3} - 5.2\frac{\bar{\Lambda}\lambda_1}{\overline{m}_B^3} - 7.9\frac{\bar{\Lambda}\lambda_2}{\overline{m}_B^3} - 0.38\frac{\bar{\Lambda}^2}{\overline{m}_B^2} - 2.06\frac{\lambda_1)}{mB^2} \\
&\quad -4.96\frac{\lambda_2}{\overline{m}_B^2} - 0.287\frac{\bar{\Lambda}}{\overline{m}_B} - 5.2\frac{\rho_1}{\overline{m}_B^3} + 1.4\frac{\rho_2}{\overline{m}_B^3} - 3.4\frac{\mathcal{T}_1}{\overline{m}_B^3} - 2.3\frac{\mathcal{T}_2}{\overline{m}_B^3} \\
&\quad -4.2\frac{\mathcal{T}_3}{\overline{m}_B^3} - 5.0\frac{\mathcal{T}_4}{\overline{m}_B^3} \\
&\quad +\frac{\alpha_s}{\pi}\left(-0.009 - 0.07\frac{\bar{\Lambda}}{\overline{m}_B}\right) + \frac{\alpha_s^2\beta_0}{\pi^2}(-0.07) + \left|\frac{V_{ub}}{V_{cb}}\right|^2\left(1.15 - 8.2\frac{\bar{\Lambda}}{\overline{m}_B}\right) \\
&\quad +\left(-0.0125 + 0.002\frac{\bar{\Lambda}}{\overline{m}_B}\right) + \left(0.0032 - 0.001\frac{\bar{\Lambda}}{\overline{m}_B}\right)
\end{aligned} \tag{4.35}$$

$$\begin{aligned}
M_2 &= 2.3360 - 1.6\frac{\bar{\Lambda}^3}{\overline{m}_B^3} - 16.0\frac{\bar{\Lambda}\lambda_1}{\overline{m}_B^3} - 22.6\frac{\bar{\Lambda}\lambda_2}{\overline{m}_B^3} - 1.14\frac{\bar{\Lambda}^2}{\overline{m}_B^2} - 7.27\frac{\lambda_1}{\overline{m}_B^2} \\
&\quad -16.21\frac{\lambda_2}{\overline{m}_B^2} - 0.989\frac{\bar{\Lambda}}{\overline{m}_B} - 20.7\frac{\rho_1}{\overline{m}_B^3} + 2.6\frac{\rho_2}{\overline{m}_B^3} - 11.4\frac{\mathcal{T}_1}{\overline{m}_B^3} - 9.5\frac{\mathcal{T}_2}{\overline{m}_B^3} \\
&\quad -13.6\frac{\mathcal{T}_3}{\overline{m}_B^3} - 16.2\frac{\mathcal{T}_4}{\overline{m}_B^3} \\
&\quad +\frac{\alpha_s}{\pi}\left(-0.049 - 0.22\frac{\bar{\Lambda}}{\overline{m}_B}\right) + \frac{\alpha_s^2\beta_0}{\pi^2}(-0.25)\left|\frac{V_{ub}}{V_{cb}}\right|^2\left(4.18 - 32.2\frac{\bar{\Lambda}}{\overline{m}_B}\right) \\
&\quad +\left(-0.0367 + 0.015\frac{\bar{\Lambda}}{\overline{m}_B}\right) + \left(0.0133 - 0.006\frac{\bar{\Lambda}}{\overline{m}_B}\right)
\end{aligned} \tag{4.36}$$

The CLEO Collaboration intends to use these moments, $R_{1,2}$, and the moments of the invariant mass spectrum to extract $\lambda_1, \bar{\Lambda}$ from experiments. Having these six measurements will shed some light on how consistent the HQET predictions for these observables are. Also, one may hope that at least some constraints on the size of the $1/m_b^3$ corrections can be obtained by demanding that the allowed regions from these six constraints overlap.

Chapter 5 Annihilation of quarkonia

5.1 Introduction

Since their discovery, heavy quarkonia have been considered an important testing ground for quantum chromodynamics [53]. By now it is well established that all qualitative features of quarkonia (e.g., a confining potential, a positronium-like spectrum, ratios of leptonic to hadronic widths) are in agreement with what we expect from QCD. However, in most cases we still do not have a fully quantitative description based on first principles. An important step towards such a description was made in Ref. [54], where a formalism of Nonrelativistic QCD (NRQCD) was proposed. It is based upon the observation that in a heavy quarkonium there are several widely separated momentum scales: the typical kinetic energy of the heavy quark, Mv^2, is much smaller than the inverse size of the quarkonium, Mv, which in turn is much smaller than the heavy quark mass M. NRQCD allows one to factor the annihilation and production rates for quarkonia into perturbatively calculable short-distance coefficients and nonperturbative long-distance matrix elements. This justifies the assumption of "naive factorization" for S-wave quarkonium. On the other hand, NRQCD elucidates the role of the higher Fock components of the quarkonium wavefunction and explains why naive factorization fails for P-wave states [54].

NRQCD provides a rigorous definition of long-distance matrix elements and thus allows, in principle, their calculation on the lattice. Still, given the immaturity of present day lattice simulations, one may ask what one can learn from quarkonia without plunging into a full-fledged lattice NRQCD computation. What we have in mind here is, first of all, a more accurate determination of α_s from the ratio of hadronic to electromagnetic widths [55]. Such a determination in particular could help to clarify the long-standing problem of a possible discrepancy between low-energy and high energy measurements of α_s [56].

In this chapter we analyze the relativistic corrections to the annihilation rates of S-wave quarkonia (both spin-singlet and spin-triplet) and apply the results of this analysis to restrict the value of α_s [57]. In Section 5.2 we show that order v^2 corrections to the color singlet part of the annihilation rate can be expressed through the mass of the quarkonium and the heavy quark pole mass. The hadronic widths of the spin-triplet states, ψ and Υ, contain also a piece due to the annihilation of the quark-antiquark pair in a color octet state. In Section 5.3 we provide a rough estimate of the latter contribution based on the running of the color octet matrix elements. These results are used in Section 5.4 to extract α_s from the ratio of hadronic to leptonic widths of $\Upsilon(1S)$.

5.2 Relativistic corrections to S-wave quarkonium annihilation rates in NRQCD

The Lagrangian of NRQCD [54] is

$$\mathcal{L}_{\rm NRQCD} = \mathcal{L}_{\rm light} + \mathcal{L}_{\rm heavy} + \delta\mathcal{L}, \tag{5.1}$$

where $\mathcal{L}_{\rm light}$ is the usual QCD Lagrangian for gluons and light quarks. $\mathcal{L}_{\rm heavy}$ is the leading term of the small velocity expansion of the QCD Lagrangian for the heavy quarks

$$\mathcal{L}_{\rm heavy} = \psi^\dagger \left(iD_t + \frac{\mathbf{D}^2}{2M} \right) \psi + \chi^\dagger \left(iD_t - \frac{\mathbf{D}^2}{2M} \right) \chi, \tag{5.2}$$

with ψ being an operator annihilating a heavy quark, and χ being an operator creating a heavy antiquark. Both ψ and χ are two component spinors that belong to the fundamental representation of the color group $SU(N_c)$. The last term, $\delta\mathcal{L}$, includes relativistic corrections to $\mathcal{L}_{\rm heavy}$ and is of order v^2 compared to it.

The annihilation of the quarkonium is a short distance process (the characteristic momentum scale is of order M) which, in the framework of NRQCD, is described by adding four-quark local operators to $\delta\mathcal{L}$. The corresponding term has the following

structure:

$$\delta\mathcal{L}_{4-\text{fermion}} = \sum_n \frac{f_n(\Lambda)}{M^{d_n-4}}\mathcal{O}_n(\Lambda), \tag{5.3}$$

where d_n is the canonical dimension of $\mathcal{O}_n$. The dimensionless coefficients $f_n(\Lambda)$ depend on the Wilsonian cutoff Λ needed to define NRQCD and can be calculated by matching the NRQCD amplitudes generated by 4-fermion terms with annihilation contributions to the scattering in full QCD. Following Ref. [54], we take $\Lambda \sim M$.

First let us collect the expressions for the decay rates of S-wave quarkonia including the first relativistic corrections. According to Ref. [54], the inclusive decay rates of η_c and η_b to light hadrons and to two photons are given by

$$\begin{aligned}
\Gamma(\eta_{c,b} \to \text{LH}) &= \frac{2\,\text{Im}\, f_1(^1S_0)}{M^2}\,\langle\eta_{c,b}|\mathcal{O}_1(^1S_0)|\eta_{c,b}\rangle \\
&\quad + \frac{2\,\text{Im}\, g_1(^1S_0)}{M^4}\,\langle\eta_{c,b}|\mathcal{P}_1(^1S_0)|\eta_{c,b}\rangle \;+\; O(v^4\Gamma), \\
\Gamma(\eta_{c,b} \to \gamma\gamma) &= \frac{2\,\text{Im}\, f_{\gamma\gamma}(^1S_0)}{M^2}\,\langle\eta_{c,b}|\mathcal{O}_1(^1S_0)|\eta_{c,b}\rangle \\
&\quad + \frac{2\,\text{Im}\, g_{\gamma\gamma}(^1S_0)}{M^4}\,\langle\eta_{c,b}|\mathcal{P}_1(^1S_0)|\eta_{c,b}\rangle \;+\; O(v^4\Gamma),
\end{aligned} \tag{5.4}$$

where $\mathcal{O}_1(^1S_0) = \psi^\dagger\chi\,\chi^\dagger\psi$, $\mathcal{P}_1(^1S_0) = 1/2\left[\psi^\dagger\chi\,\chi^\dagger(-\frac{i}{2}\overleftrightarrow{\mathbf{D}})^2\psi \;+\; \text{h.c.}\right]$.

For the spin-triplet S-states, ψ and Υ, the situation is more complicated. The leading term and the order v^2 relativistic correction to the $\ell^+\ell^-$ decay rate are proportional to the expectation values of $\mathcal{O}_1(^3S_1) = \psi^\dagger\boldsymbol{\sigma}\chi\cdot\chi^\dagger\boldsymbol{\sigma}\psi$ and $\mathcal{P}_1(^3S_1) = \frac{1}{2}\left[\psi^\dagger\boldsymbol{\sigma}\chi\cdot\chi^\dagger\boldsymbol{\sigma}(-\frac{i}{2}\overleftrightarrow{\mathbf{D}})^2\psi \;+\; \text{h.c.}\right]$ respectively:

$$\Gamma(\Upsilon \to \ell^+\ell^-) = \frac{2\,\text{Im}\, f_{ee}(^3S_1)}{M^2}\,\langle\Upsilon|\mathcal{O}_1(^3S_1)|\Upsilon\rangle + \frac{2\,\text{Im}g_{ee}(^3S_1)}{M^4}\,\langle\Upsilon|\mathcal{P}_1(^3S_1)|\Upsilon\rangle. \tag{5.5}$$

The decay rate of ψ or Υ to light hadrons receives contributions from both color-singlet and color octet components of the quarkonium wavefunction. The color-singlet component can only decay into three or more gluons. In contrast, the color octet component can decay into two gluons or into a virtual gluon which then creates a quark-antiquark pair (see Fig. 5.1). Hence, the color octet contribution is of order

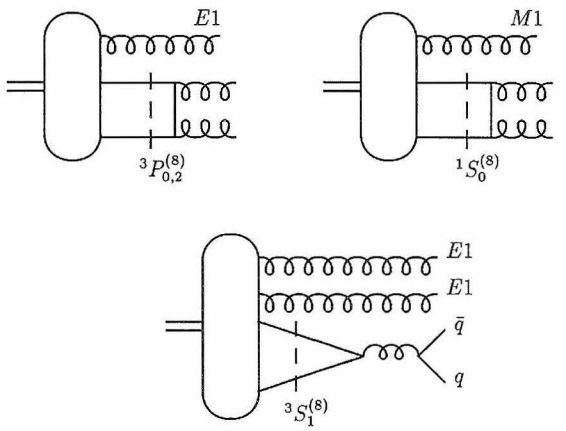

Figure 5.1: Contributions of higher Fock states to the hadronic annihilation of spin-1 S-wave quarkonia. All diagrams shown here contribute to the rate at order $\alpha_s^2 v^4$.

$\alpha_s^2 v^4$ and may compete with the relativistic correction to the color-singlet rate which is of order $\alpha_s^3 v^2$. (We will see in the next section that this color octet contribution is essential for explaining experimental data on Υ decays.) Therefore, the inclusive rate to light hadrons is

$$\begin{aligned}\Gamma(\Upsilon \to \mathrm{LH}) &= \frac{2\,\mathrm{Im}\, f_1(^3S_1)}{M^2}\,\langle\Upsilon|\mathcal{O}_1(^3S_1)|\Upsilon\rangle + \frac{2\,\mathrm{Im} g_1(^3S_1)}{M^4}\,\langle\Upsilon|\mathcal{P}_1(^3S_1)|\Upsilon\rangle \\ &\quad + \Gamma^{(8)}(\Upsilon \to \mathrm{LH}).\end{aligned} \tag{5.6}$$

The color octet part of the decay rate $\Gamma^{(8)}(\Upsilon \to \mathrm{LH})$ receives contributions from three four-quark operators corresponding to the three diagrams in Fig. 5.1:

$$\begin{aligned}\Gamma^{(8)}(\Upsilon \to \mathrm{LH}) &= \frac{2\,\mathrm{Im}\,(f_8(^3P_0) + 5 f_8(^3P_2))}{M^4}\,\langle\Upsilon|\mathcal{O}_8(^3P_0)|\Upsilon\rangle + \\ &\quad + \frac{2\,\mathrm{Im}\, f_8(^1S_0)}{M^2}\,\langle\Upsilon|\mathcal{O}_8(^1S_0)|\Upsilon\rangle \\ &\quad + \frac{2\,\mathrm{Im}\, f_8(^3S_1)}{M^2}\,\langle\Upsilon|\mathcal{O}_8(^3S_1)|\Upsilon\rangle.\end{aligned} \tag{5.7}$$

In the latter equation we have used heavy quark spin symmetry to reexpress the expectation value of $\mathcal{O}_8(^3P_2)$ in terms of $\mathcal{O}_8(^3P_0)$. The color octet operators are

defined as

$$\begin{aligned}
\mathcal{O}_8(^3P_0) &= \frac{1}{3}\,\psi^\dagger T^a(-\tfrac{i}{2}\overleftrightarrow{\mathbf{D}}\cdot\boldsymbol{\sigma})\chi\,\chi^\dagger T^a(-\tfrac{i}{2}\overleftrightarrow{\mathbf{D}}\cdot\boldsymbol{\sigma})\psi,\\
\mathcal{O}_8(^1S_0) &= \psi^\dagger T^a\chi\,\chi^\dagger T^a\psi,\\
\mathcal{O}_8(^3S_1) &= \psi^\dagger\boldsymbol{\sigma}T^a\chi\cdot\chi^\dagger\boldsymbol{\sigma}T^a\psi. \qquad (5.8)
\end{aligned}$$

The short-distance coefficients in the expressions for the decay rates Eqs. (5.4-5.7) depend on the scheme adopted to define the operators. We wish to derive relations between the matrix elements of the operators $\mathcal{P}_1(^1S_0), \mathcal{P}_1(^3S_1)$ and $\mathcal{O}_1(^1S_0), \mathcal{O}_1(^3S_1)$, which can be used to express the decay rates including the first relativistic corrections through the leading order matrix elements. Since these relations also depend on the choice of the scheme, we will discuss this issue in some detail here. We will limit our discussion to the operators appearing in the decay rate of the $\eta_{b,c}$. An identical argument can be made for the operators appearing in the decay rates of the Υ and ψ.

The vacuum saturation approximation provides the following estimate for the matrix element of $\mathcal{P}_1(^1S_0)$

$$\langle\eta_{c,b}|\mathcal{P}_1(^1S_0)|\eta_{c,b}\rangle = \frac{1}{2}\mathrm{Re}\,\langle\eta_{c,b}|\psi^\dagger\chi|0\rangle\langle 0|\left((i\mathbf{D})^2\chi\right)^\dagger\psi+\chi^\dagger\left(i\mathbf{D}\right)^2\psi|\eta_{c,b}\rangle. \quad (5.9)$$

The operator with two derivatives in this expression is not defined unambiguously beyond tree level; for example, one is free to perform a shift

$$\begin{aligned}
\left(\left((i\mathbf{D})^2\chi\right)^\dagger\psi+\chi^\dagger\left(i\mathbf{D}\right)^2\psi\right)_\Lambda \;\rightarrow\; &\left(\left((i\mathbf{D})^2\chi\right)^\dagger\psi+\chi^\dagger\left(i\mathbf{D}\right)^2\psi\right)_\Lambda \qquad (5.10)\\
&+C(\Lambda,M)\left(\chi^\dagger\psi\right)_\Lambda.
\end{aligned}$$

Here Λ is the Wilsonian cutoff, and $C(\Lambda, M)$ is a power series in α_s starting with a term of order α_s. (In what follows we will omit the subscript Λ, with the understanding that all operators are regularized using the Wilsonian cutoff.) Among all

possible definitions of the operator with two derivatives, only a subset satisfies the NRQCD velocity counting rules. According to these rules, the matrix element of the operator with two derivatives should scale as $\mathbf{p}^2$ relative to the matrix element of $\chi^\dagger\psi$ as $\mathbf{p} \to 0$:

$$\frac{\langle 0|\left((i\mathbf{D})^2\chi\right)^\dagger\psi + \chi^\dagger(i\mathbf{D})^2\psi|\mathbf{p},-\mathbf{p}\rangle}{\langle 0|\chi^\dagger\psi|\mathbf{p},-\mathbf{p}\rangle} = \mathcal{O}(\mathbf{p}^2). \tag{5.11}$$

Here $|\mathbf{p},-\mathbf{p}\rangle$ is an asymptotic quark-antiquark state with momenta $\mathbf{p}$ and $-\mathbf{p}$. Imposing this condition removes the freedom to redefine the operator as in Eq. (5.10).

With the convention Eq. (5.11) it is particularly simple to determine the short-distance coefficient of the operator $\mathcal{O}_1(^1S_0)$ at next-to-leading order (NLO) by comparing the v^{-1} and v^0 contributions in full QCD and NRQCD. On the NRQCD side it is sufficient to calculate the annihilation of a quark-antiquark pair via the operator $\mathcal{O}_1(^1S_0)$. The choice Eq. (5.11) guarantees that there are no NLO contributions from the operator $\mathcal{P}_1(^1S_0)$ proportional to v^{-1} or v^0.

Other ways of defining the operators are, of course, possible. If the $\mathbf{p} \to 0$ limit of the expression on the right-hand side of Eq. (5.11) is nonzero, the operator $\mathcal{P}_1(^1S_0)$ will contribute to the annihilation rate at order v^{-1} and v^0. In this case one needs to know the leading order short-distance coefficient of $\mathcal{P}_1(^1S_0)$ in order to determine that of $\mathcal{O}_1(^1S_0)$ at NLO. In fact, unless one requires operators with arbitrarily many derivatives to satisfy conditions similar to Eq. (5.11), they all have to be taken into account in the computation of the short-distance coefficient of $\mathcal{O}_1(^1S_0)$ to next-to-leading order.

In Ref. [54] it was assumed that the operators with two or more derivatives need not be taken into account when computing the NLO short-distance coefficient of $\mathcal{O}_1(^1S_0)$. In other words, it is implicit in Ref. [54] that the scaling behavior of the operators is given by the NRQCD counting rules or, equivalently, that Eq. (5.11) and similar equations for operators with more derivatives are satisfied. We adopt the same convention here.

The equations of motion for the quark fields to leading order in v^2 are

$$\left(iD_t + \frac{\mathbf{D}^2}{2M}\right)\psi = 0, \qquad \left(iD_t - \frac{\mathbf{D}^2}{2M}\right)\chi = 0. \tag{5.12}$$

They can be used to trade the spatial derivatives in the operator with two derivatives in Eq. (5.9) for time derivatives acting on the quark fields:

$$\left[\left((i\mathbf{D})^2\chi\right)^\dagger\psi + \chi^\dagger(i\mathbf{D})^2\psi\right] + A(\Lambda, M)\,\chi^\dagger\psi \;=\; 2M\,i\partial_t\left(\chi^\dagger\psi\right). \tag{5.13}$$

Here A is a scheme dependent coefficient whose expansion in powers of α_s starts, in general, with the term of order α_s. The term proportional to $\chi^\dagger\psi$ has to be included in the relation Eq. (5.13), because $\chi^\dagger\psi$ mixes into the operator with two derivatives under shifts as in Eq. (5.10). There are corrections to Eq. (5.13) at higher orders in v^2, but for our purposes it is sufficient to take into account only the terms shown.

Let us show that with the convention Eq. (5.11), $A(\Lambda, M)$ is zero to all orders in α_s. Evaluating Eq. (5.13) between vacuum and a quark-antiquark state $|\mathbf{p}, -\mathbf{p}\rangle$ yields:

$$\langle 0|\left((i\mathbf{D})^2\chi\right)^\dagger\psi + \chi^\dagger(i\mathbf{D})^2\psi|\mathbf{p}, -\mathbf{p}\rangle = \left(2\mathbf{p}^2 - A(\Lambda, M)\right)\langle 0|\chi^\dagger\psi|\mathbf{p}, -\mathbf{p}\rangle. \tag{5.14}$$

We have used the identity

$$\langle 0|i\partial_t\left(\chi^\dagger\psi\right)|\mathbf{p}, -\mathbf{p}\rangle = \langle 0|\left[\chi^\dagger\psi,\, H\right]|\mathbf{p}, -\mathbf{p}\rangle = \frac{\mathbf{p}^2}{M}\langle 0|\chi^\dagger\psi|\mathbf{p}, -\mathbf{p}\rangle, \tag{5.15}$$

where H is the NRQCD Hamiltonian. The identity Eq. (5.15) holds to all orders in α_s, because the asymptotic state $|\mathbf{p}, -\mathbf{p}\rangle$ is an eigenstate of H with eigenvalue $\mathbf{p}^2/M$. Dividing both sides of Eq. (5.14) by $\langle 0|\chi^\dagger\psi|\mathbf{p}, -\mathbf{p}\rangle$, taking the limit $\mathbf{p} \to 0$ and using Eq. (5.11), one sees that $A(\Lambda, M) = 0$.

Taking the expectation value of Eq. (5.13) with $A = 0$ yields the following relation:

$$\langle\eta_{c,b}|\mathcal{P}_1(^1S_0)|\eta_{c,b}\rangle \;=\; \frac{1}{2}\mathrm{Re}\,\langle\eta_{c,b}|\psi^\dagger\chi|0\rangle\langle 0|\left((i\mathbf{D})^2\chi\right)^\dagger\psi + \chi^\dagger(i\mathbf{D})^2\psi|\eta_{c,b}\rangle$$

$$
\begin{aligned}
&= M\mathrm{Re}\,\langle\eta_{c,b}|\psi^\dagger\chi|0\rangle\langle 0|i\partial_t\left(\chi^\dagger\psi\right)|\eta_{c,b}\rangle\left(1+O(v^2)\right)\\
&= ME_{\eta_{c,b}}\langle\eta_{c,b}|\mathcal{O}_1(^1S_0)|\eta_{c,b}\rangle\left(1+O(v^2)\right). \qquad (5.16)
\end{aligned}
$$

Here $E_{\eta_{c,b}}$ is the energy of the quarkonium state. Since in NRQCD the rest mass of the quarks is not included in the energy of a quarkonium state, we can express $E_{\eta_{c,b}}$ in terms of the mass of the $\eta_{b,c}$ and the quark pole mass

$$E_{\eta_{c,b}} = M_{\eta_{b,c}} - 2M. \qquad (5.17)$$

Eqs. (5.16) and (5.17), and similar relations for the operators in the spin-triplet decay rates, allow us to express the relativistic corrections to the decay rates in terms of the leading order matrix elements and the "binding energy" of the quarkonium $M_{q\bar{q}}-2M_q$. For example, the decay rate of the Υ to light hadrons now takes the form

$$
\begin{aligned}
\Gamma(\Upsilon\to\mathrm{LH}) &= \frac{2\,\mathrm{Im}\,f_1(^3S_1)}{M^2}\langle\Upsilon|\mathcal{O}_1(^3S_1)|\Upsilon\rangle\left(1+\frac{M_\Upsilon-2M}{M}\frac{\mathrm{Im}\,g_1(^3S_1)}{\mathrm{Im}\,f_1(^3S_1)}\right)\\
&+ \Gamma^{(8)}(\Upsilon\to\mathrm{LH}), \qquad (5.18)
\end{aligned}
$$

and similar expressions hold for the other decay rates Eqs. (5.4) and Eq. (5.5).

All coefficients in Eqs. (5.4) and Eqs. (5.5-5.7), except $f_8(^3P_0)$, $f_8(^3P_2)$, and $g_1(^3S_1)$, have been calculated to the necessary order in α_s in Ref. [54]. The coefficients $f_8(^3P_0)$, $f_8(^3P_2)$ can be extracted from Eqs. (A9-A13) of Ref. [54]:

$$\mathrm{Im}f_8(^3P_0) = \frac{3\pi(N_c^2-4)}{4N_c}\alpha_s^2(M), \quad \mathrm{Im}f_8(^3P_2) = \frac{\pi(N_c^2-4)}{5N_c}\alpha_s^2(M). \qquad (5.19)$$

To extract $g_1(^3S_1)$ to leading order in α_s we need to compute the three-gluon annihilation rate of a free quark-antiquark pair to order v^2 in their relative velocity. Fortunately, this computation has already been performed in the context of e^+e^- annihilation [58]. We have checked the results quoted in these papers. The annihilation

rate of a free quark-antiquark pair in a spin triplet state to order v^2 turns out to be

$$\Gamma\left(q\bar{q}(^3S_1) \to 3g, v\right) = \Gamma\left(q\bar{q}(^3S_1) \to 3g, 0\right)\left[1 - v^2\frac{19\pi^2 - 132}{12\pi^2 - 108} + O(v^4)\right], \quad (5.20)$$

where $\Gamma\left(q\bar{q}(^3S_1) \to 3g, v\right)$ represents the annihilation rate of the quark-antiquark pair in a spin-triplet state, with v denoting the velocity of the quark in the center of mass frame. Comparing with the corresponding amplitude in NRQCD, we obtain

$$\frac{\mathrm{Im}\, g_1(^3S_1)}{\mathrm{Im}\, f_1(^3S_1)} = -\frac{19\pi^2 - 132}{12\pi^2 - 108}\left(1 + O(\alpha_s)\right). \quad (5.21)$$

One consequence of the last equation is that for the spin-triplet states the order v^2 relativistic correction to the hadronic rate is unexpectedly large. For the b quark pole mass in the range $4.6 - 4.9$ GeV, the correction to the $\Upsilon(1S)$ decay rate can be as large as 25%, and still bigger for radially excited states. For $m_c^{pole} \simeq 1.3$ GeV, the correction to the J/ψ hadronic decay rate is about 150%. Its magnitude makes one question the usefulness of the nonrelativistic expansion for charmonium. For spin-singlet states, the relativistic corrections are of the expected size.

5.3 Estimates of the color octet matrix elements

In order to use our expressions for phenomenological applications, estimates for the color octet contributions are needed. Following Ref. [54], we can obtain very rough estimates by solving the renormalization group equations for the color octet operators. To order v^4 and leading order in α_s we find

$$\begin{aligned}
\Lambda\frac{d}{d\Lambda}\langle\Upsilon|\mathcal{O}_8(^1S_0)|\Upsilon\rangle &= 0, \\
\Lambda\frac{d}{d\Lambda}\langle\Upsilon|\mathcal{O}_8(^3S_1)|\Upsilon\rangle &= \frac{4(N_c^2-4)\alpha_s}{N_c\pi M^2}\langle\Upsilon|\mathcal{O}_8(^3P_0)|\Upsilon\rangle, \\
\Lambda\frac{d}{d\Lambda}\langle\Upsilon|\mathcal{O}_8(^3P_0)|\Upsilon\rangle &= \frac{4C_F\alpha_s}{81N_c\pi}(M_\Upsilon - 2M)^2\langle\Upsilon|\mathcal{O}_1(^3S_1)|\Upsilon\rangle,
\end{aligned} \quad (5.22)$$

where

$$\langle\Upsilon|\psi^\dagger\boldsymbol{\sigma}(-\tfrac{i}{2}\overleftrightarrow{\mathbf{D}})^2\chi\chi^\dagger\boldsymbol{\sigma}(-\tfrac{i}{2}\overleftrightarrow{\mathbf{D}})^2\psi|\Upsilon\rangle = M^2(M_\Upsilon - 2M)^2\langle\Upsilon|\mathcal{O}_1(^3S_1)|\Upsilon\rangle \tag{5.23}$$

was used in Eqs. (5.22). We can express the matrix elements at the factorization scale $\Lambda \sim M$ in terms of those at a low scale $\Lambda \sim \Lambda_{\rm QCD}$ by solving Eqs. (5.22). The color octet operators mix between themselves and with color-singlet operators. Formally, the terms coming from the mixing with color-singlets are logarithmically enhanced. To get a rough estimate of the color octet matrix elements, we assume that these terms dominate. This yields:

$$\begin{aligned}
\langle\Upsilon|\mathcal{O}_8(^3S_1)|\Upsilon\rangle &\approx \frac{8(N_c^2-4)C_F}{81N_C^2\pi^2}\frac{(M_\Upsilon-2M)^2}{M^2}\left(\frac{2\pi}{\beta_0}\ln\left(\frac{1}{\alpha_s(M)}\right)\right)^2 \\
&\quad\times\langle\Upsilon|\mathcal{O}_1(^3S_1)|\Upsilon\rangle, \qquad (5.24)\\
\langle\Upsilon|\mathcal{O}_8(^3P_0)|\Upsilon\rangle &\approx \frac{4C_F}{81N_c\pi}(M_\Upsilon-2M)^2\,\frac{2\pi}{\beta_0}\ln\left(\frac{1}{\alpha_s(M)}\right)\langle\Upsilon|\mathcal{O}_1(^3S_1)|\Upsilon\rangle. \qquad (5.25)
\end{aligned}$$

In the same spirit we set $\langle\Upsilon|\mathcal{O}_8(^1S_0)|\Upsilon\rangle \approx 0$ since it does not acquire a logarithmically enhanced contribution.

In order to check whether these estimates are reasonable, we consider the following "ratio of ratios":

$$R_{mn}(\Upsilon) = \frac{\Gamma\left(\Upsilon(mS)\to \mathrm{LH}\right)/\Gamma\left(\Upsilon(mS)\to \ell^+\ell^-\right)}{\Gamma\left(\Upsilon(nS)\to \mathrm{LH}\right)/\Gamma\left(\Upsilon(nS)\to \ell^+\ell^-\right)}. \tag{5.26}$$

Substituting Eq. (5.7) and a similar expression for the dileptonic rate into Eq. (5.26) we get

$$R_{mn} = 1 - 8.0\frac{M_m - M_n}{M_m} + \frac{\Gamma^{(8)}\left(\Upsilon(mS)\to \mathrm{LH}\right)}{\Gamma\left(\Upsilon(mS)\to \mathrm{LH}\right)} - \frac{\Gamma^{(8)}\left(\Upsilon(nS)\to \mathrm{LH}\right)}{\Gamma\left(\Upsilon(nS)\to \mathrm{LH}\right)} + O(v^4, \alpha_s v^2). \tag{5.27}$$

Neglecting the color octet contribution completely, we obtain $R_{12} \simeq 1.5$, in disagreement with the experimental value $R_{12} = 0.95 \pm 0.15$ [59]. In order to evaluate the color octet contribution numerically, we need the pole mass of the b quark. Various

methods give M in the range $4.6-4.9$ GeV [60, 8, 9, 61] corresponding to the theoretical value $R_{12} \simeq 0.95-1.53$. For the lower quark masses, our estimates shift the value of R_{12} much closer to the experimental number. We take this to be an indication that our estimates give reasonable order of magnitude values for the color octet matrix elements.

5.4 Application to the determination of α_s

As we have seen in the previous section, the leading relativistic correction to the annihilation rates of η_c and η_b is expressed in terms of the b quark pole mass. The latter can be extracted from the measurement of moments of the photon spectrum in the inclusive $b \to s\gamma$ decay [29], from inclusive semileptonic $b \to c$ decays [60, 8, 9], or from sum rules for quarkonia [61]. Therefore, the ratios of hadronic to radiative decay rates of η_c and η_b are ideal for determining α_s. Unfortunately, these measurements are very hard (though not impossible) to do[3]. The Υs are much easier to study from the experimental point of view, but the theoretical interpretation is complicated by the presence of the color octet contribution. We use the results of the previous section to estimate this contribution to the hadronic decay rate. For $M = 4.6 - 4.9$ GeV the color octet contribution ranges from 0 to 9%. Therefore, we take 9% as an estimate of the error from neglecting it. The order v^2 relativistic correction is evaluated with M in the same range as above. We use the renormalization scale dependence of the NLO prediction to estimate the error from perturbative NNLO corrections.

Having adopted such estimates of theoretical uncertainties, we use the experimental value $\Gamma\left(\Upsilon(1S) \to \mathrm{LH}\right)/\Gamma\left(\Upsilon(1S) \to \ell^+\ell^-\right) = 37.3 \pm 1.0$ [59], to determine $\alpha_s(M) = 0.154 - 0.218$. This corresponds to

$$\alpha_s(M_Z) = 0.097 - 0.117 \tag{5.28}$$

[3]There is still one problem on the theoretical side. Next-to-leading order (NLO) perturbative corrections to these ratios are very large [54, 62], and one would like to know NNLO corrections to have some idea about the convergence of the perturbation series.

at the scale M_Z. The higher value of $\alpha(M_Z)$ corresponds to the lower value of the b quark pole mass. This range for $\alpha_s(M_Z)$ overlaps with the 1 σ confidence interval of the LEP measurement $\alpha_s(M_Z) = 0.120 \pm 0.004$ [63]. The accuracy of our extraction being limited by theoretical uncertainties, the range in Eq. (5.28) should not be interpreted as a 1 σ error. We do not quote here the values of α_s obtained from $\Upsilon(2S)$ decays because the theoretical uncertainties are much larger, and also because the accuracy of data on $\Upsilon(2S)$ is worse.

Further improvements in this determination of α_s would come from a more accurate extraction of the b quark pole mass, and also from a NNLO perturbative calculation of the short-distance coefficient $\mathrm{Im}\, f_1(^3S_1)$. For example, knowledge of the pole mass to within 50 MeV would reduce the uncertainties roughly by a factor of two.

5.5 Conclusions

We have shown that order v^2 relativistic corrections to annihilation rates of the S-wave quarkonia can be expressed in terms of the quarkonium "binding energy." For spin-singlet states this observation makes it possible to predict accurately the ratio of hadronic to radiative decay rates in terms of α_s and the heavy quark pole mass. However, a calculation of the NNLO perturbative contributions to the short-distance coefficients is necessary to ensure that perturbative corrections are under control. For spin-triplet states, which are much more accessible experimentally, the color octet component of the quarkonium wavefunction may contribute significantly to the hadronic annihilation rate, although the corresponding contributions are of order v^4 in the nonrelativistic expansion. Therefore, knowledge of the expectation values of color octet operators is needed, if we want to predict the hadronic to leptonic ratio for spin-triplet quarkonia. We used crude estimates based on renormalization group equations to deduce the uncertainties due to the color octet contributions. From the experimental data on the $\Upsilon(1S)$ decays, we extract $\alpha_s(M_Z) = 0.097 - 0.117$, the major part of the uncertainty coming from the uncertainty in the b quark pole mass.

Further experimental and theoretical efforts are needed to obtain a better estimate of α_s from quarkonia decays.

Chapter 6 Concluding remarks

We have shown two applications of effective field theories in QCD. In the first part of this thesis we introduced Heavy Quark Effective Theory and used it to describe the inclusive semileptonic weak decay of B mesons to charmed final states. HQET allows one to parametrize the nonperturbative corrections to the quark level decay rate in terms of a small number of matrix elements and measurable quantities such as the meson masses. Specifically, the leading corrections can be expressed in terms of $\bar{\Lambda}$, λ_1 and λ_2, where λ_2 is fixed by the $B-B^*$ mass splitting. Moments of the charged lepton or hadronic invariant mass spectrum can be used to extract the values of the two unknown HQET parameters from experimental data. The theoretical uncertainties in this extraction are unfortunately rather large. This is mainly due to higher order HQET corrections. The problem is not that these corrections are abnormally large. Because the different observables we construct from the lepton spectrum give almost the same constraints in the $\bar{\Lambda} - \lambda_1$ plane, even small corrections can change the extracted values substantially. However, there is one linear combination of $\bar{\Lambda}$ and λ_1 that is fairly well constrained even if the uncertainties from higher order matrix elements are taken into account. We also consider the perturbative corrections of order $\alpha_s^2\beta_0$ to the lepton spectrum. While the resulting corrections to the moments of the electron spectrum are huge, the extracted value of $\bar{\Lambda}$ and λ_1 is shifted only by a small amount relative to the values extracted without the $\alpha_s^2\beta_0$ corrections. This suggests that this method of extracting these HQET parameters is not very sensitive to perturbative corrections. The main theoretical uncertainties are certainly due to the higher order nonperturbative corrections.

Once the values of $\bar{\Lambda}$ and λ_1 are extracted, one can use them to determine the weak mixing angle V_{cb} and the b and c pole quark masses, albeit with relatively large uncertainties. These uncertainties could be reduced if some constraints on $\bar{\Lambda}$ and λ_1 from other decays were available. Such constraints would probably differ from the

constraints from semileptonic B decays, i.e., constrain a different linear combination of $\bar{\Lambda}$ and λ_1. The most promising candidate is the photon spectrum in $B \to X_s\gamma$ but so far there is not enough experimental data to get useful constraints from this decay.

Nonrelativistic QCD is an effective field theory in which the properties of heavy quarkonia can be studied. We consider the annihilation rates of S-wave quarkonia into light hadrons and two leptons including the first relativistic corrections. These corrections can be expressed in terms of the leading order matrix elements and the quark pole mass. Using our results from the HQET analysis, we find that the relativistic corrections are significant in the $b\bar{b}$ system and extremely large in some of the $c\bar{c}$ decays. Also, by comparing NRQCD predictions to measured quantities, we find that the color octet contributions cannot be neglected. Focusing on the Υ system, we use the annihilation rates including the relativistic corrections and the color octet contributions to determine α_s from low energy data. Our value agrees within errors with the LEP determination at high energies. This indicates that maybe there is no marked disparity between low and high energy determinations of α_s.

Bibliography

[1] N. Isgur and M.B. Wise, Phys. Lett. B232 (1989) 113; Phys. Lett. B237 (1990) 527.

[2] E. Eichten and B. Hill, Phys. Lett. B234 (1990) 511; H. Georgi, Phys. Lett. B240 (1990) 447.

[3] A.V. Manohar and M.B. Wise, Phys. Rev. D49 (1994) 1310.

[4] I.I. Bigi, N.G. Uraltsev, and A.I. Vainshtein, Phys. Lett. B293 (1992) 430 [(E) Phys. Lett. B297 (1993) 477]; I.I. Bigi, M. Shifman, N.G. Uraltsev, and A. Vainshtein, Phys. Rev. Lett. 71 (1993) 496; B. Blok, L. Koyrakh, M. Shifman and A.I. Vainshtein, Phys. Rev. D49 (1994) 3356.

[5] S. Balk, J.G. Körner, and D. Pirjol, Nucl. Phys. B428 (1994) 499.

[6] M. Luke and A.V. Manohar, Phys. Lett. B286 (1992) 348; Yu-Qi Chen, Phys. Lett. B317 (1993) 421; W. Kilian and T. Ohl, Phys. Rev. D50 (1994) 4649; M. Finkemeier, H. Georgi, and M. McIrvin, preprint HUTP-96-A053 [hep-ph/9701243], to be published in Phys. Rev. D; R. Sundrum, preprint BUHEP-97-14 [hep-ph/9704256].

[7] G.P. Lepage and B.A. Thacker, Nucl. Phys. B (Proc. Suppl.) 4 (1988) 199; E. Eichten and B. Hill, Phys. Lett. B243 (1990) 427; A.F. Falk, B. Grinstein and M.E. Luke, Nucl. Phys. B357 (1991) 185.

[8] M. Gremm, A. Kapustin, Z. Ligeti, and M.B. Wise, Phys. Rev. Lett. 77 (1996) 20.

[9] M. Gremm and A. Kapustin, Phys. Rev. D55 (1997) 6924.

[10] M. Gremm and I. Stewart, Phys. Rev. D55 (1997) 1226.

[11] J. Chay, H. Georgi, and B. Grinstein, Phys. Lett. B247 (1990) 399; M. Voloshin and M. Shifman, Sov. J. Nucl. Phys. 41 (1985) 120.

[12] I.I. Bigi, M. Shifman, N.G. Uraltsev, and A. Vainshtein, Phys. Rev. D52 (1995) 196.

[13] T. Mannel, Nucl. Phys. B413 (1994) 396.

[14] T. Mannel, Phys. Rev. D50 (1994) 428.

[15] A.L. Fetter and J.D. Walecka, Quantum theory of many-particle systems, McGraw-Hill, 1971.

[16] B. Blok, R.D. Dikeman, and M. Shifman, Phys. Rev. D51 (1995) 6167.

[17] M. Jezabek and J.H. Kuhn, Nucl. Phys. B320 (1989) 20; A. Czarnecki and M. Jezabek, Nucl. Phys. B427 (1994) 3.

[18] B.H. Smith and M.B. Voloshin, Phys. Lett. B340 (1994) 176.

[19] M. Luke, M.J. Savage, and M.B. Wise, Phys. Lett. B343 (1995) 329; M. Luke, M.J. Savage, and M.B. Wise, Phys. Lett. B345 (1995) 301.

[20] A. Czarnecki, Phys. Rev. Lett. 76 (1996) 4124.

[21] S.J. Brodsky, G.P. Lepage, and P.B. Mackenzie, Phys. Rev. D28 (1983) 228.

[22] G.'t Hooft and M. Veltman, Nucl. Phys. B153 (1979) 365; G. Passarino and M. Veltman, Nucl. Phys. B160 (1979) 151.

[23] M. Luke, Phys. Lett. B252 (1990) 447.

[24] H. Georgi, B. Grinstein, and M.B. Wise, Phys. Lett. B252 (1990) 456.

[25] N. Cabibbo, G. Corbo, and L. Maiani, Nucl. Phys. B155 (1979) 93; G. Altarelli, N. Cabibbo, G. Corbo, and L. Maiani, Nucl. Phys. B208 (1982) 365.

[26] M. Neubert, Phys. Rev. D46 (1992) 1076; E. Bagan *et al.*, Phys. Lett. B278 (1992) 457; V. Eletsky and E. Shuryak, Phys. Lett. B276 (1992) 191; P. Ball and V. M. Braun, Phys. Rev. D49 (1994) 2472.

[27] M. Luke and M.J. Savage, Phys. Lett. B321 (1994) 88.

[28] Z. Ligeti and Y. Nir, Phys. Rev. D49 (1994) 4331.

[29] A. Kapustin and Z. Ligeti, Phys. Lett. B355 (1995) 318.

[30] A.F. Falk, M. Luke, and M. Savage, Phys. Rev. D53 (1996) 2491; Phys. Rev. D53 (1996) 6316.

[31] A. Kapustin, Z. Ligeti, M.B. Wise, and B. Grinstein, Phys. Lett. B375 (1996) 327.

[32] J. Bartelt *et al.*, CLEO Collaboration, CLEO/CONF 93-19.

[33] B. Barish *et al.*, CLEO Collaboration, CLEO 95-17.

[34] R. Wang, Ph.D. Thesis, University of Minnesota (1994).

[35] D. Atwood and W.J. Marciano, Phys. Rev. D41 (1990) 1736.

[36] Y. Kubota *et al.*, CLEO Collaboration, Nucl. Instr. and Meth. A320 (1992) 66.

[37] R. Wang, private communications.

[38] M.B. Voloshin, Phys. Rev. D51 (1995) 4934.

[39] I.I. Bigi, M. Shifman, N. Uraltsev, and A. Vainshtein, Phys. Rev. D50 (1994) 2234; M. Beneke and V.M. Braun, Nucl. Phys. B426 (1994) 301.

[40] M. Beneke, V. Braun, and V. Zakharov, Phys. Rev. Lett. 73 (1994) 3058; M. Luke, A. Manohar, and M. Savage, Phys. Rev. D51 (1995) 4924; M. Neubert and C.T. Sachrajda, Nucl. Phys. B438 (1995) 235.

[41] M. Crisafulli, V. Gimenez, G. Martinelli, and C.T. Sachrajda, Nucl. Phys. B457 (1995) 594; C. Davies et al., Phys. Rev. Lett. 73 (1994) 2654.

[42] G. Martinelli and C.T. Sachrajda, preprint hep-ph/9605336.

[43] G. Martinelli, M. Neubert, and C.T. Sachrajda, Nucl. Phys. B461 (1996) 238.

[44] N. Isgur, D. Scora, B. Grinstein, and M. Wise, Phys. Rev. D39 (1989) 799.

[45] D. Scora and N. Isgur, Phys. Rev. D52 (1995) 2783.

[46] I.I. Bigi, M. Shifman, N.G. Uraltsev, and A. Vainshtein, Int. J. Mod. Phys. A9 (1994) 2467.

[47] C.K. Chow and D. Pirjol, Phys. Rev. D53 (1996) 3998.

[48] M.A. Shifman and M.B. Voloshin, Sov. J. Nucl. Phys. 45 (1987) 292; M.B. Voloshin, N.G. Uraltsev, V.A. Khoze and M.A. Shifman, Sov. J. Nucl. Phys. 46 (1987) 112.

[49] V. Chernyak, Phys. Lett. B387 (1996) 173.

[50] ALEPH Collaboration, contributed paper to ICHEP96, reference pa01-073.

[51] T.E. Browder et al., CLEO CONF 96-2, contributed paper to ICHEP96, reference pa05-077.

[52] R. Akers et al., Z.Phys. C67 (1995) 57.

[53] T. Applequist and H. D. Politzer, Phys. Rev. Lett. 34 (1975) 43; see also W. Buchmüller, ed., Quarkonia, North-Holland, 1992.

[54] G. T. Bodwin, E. Braaten, and G. P. Lepage, Phys. Rev. D51 (1995) 1125 (erratum hep-ph/9407339).

[55] I. Hinchliffe, Quantum Chromodynamics, in: L. Montanet *et al.*, Review of Particle Properties, Phys. Rev. D54 (1996) 77.

[56] M. Shifman, Mod. Phys. Lett. A10 (1995) 605.

[57] M. Gremm and A. Kapustin, Phys. Lett. B407 (1997) 323.

[58] E.A. Kuraev, T.V. Kuhto, and Z.K. Silagadze, Sov. J. Nucl. Phys. 51 (1990) 1036;
P. Labelle, G.P. Lepage, and U. Magnea, Order $m\alpha^8$ contributions to the decay rate of orthopositronium, hep-ph/9310208.

[59] L. Montanet *et al.*, Review of Particle Properties, Phys. Rev. D54 (1996) 1.

[60] A. F. Falk, M. Luke, and M. J. Savage, Phys. Rev. D53 (1996) 6316.

[61] S. Narison, Phys. Lett. B341 (1994) 73, M. B. Voloshin, Int. J. Mod. Phys. A10 (1995) 2865.

[62] R. Barbieri, G. Curci, E. d'Emilio, and E. Remiddi, Nucl. Phys. B154 (1979) 535.

[63] G. Altarelli, Status of precision tests of the Standard Model, hep-ph/9611239.